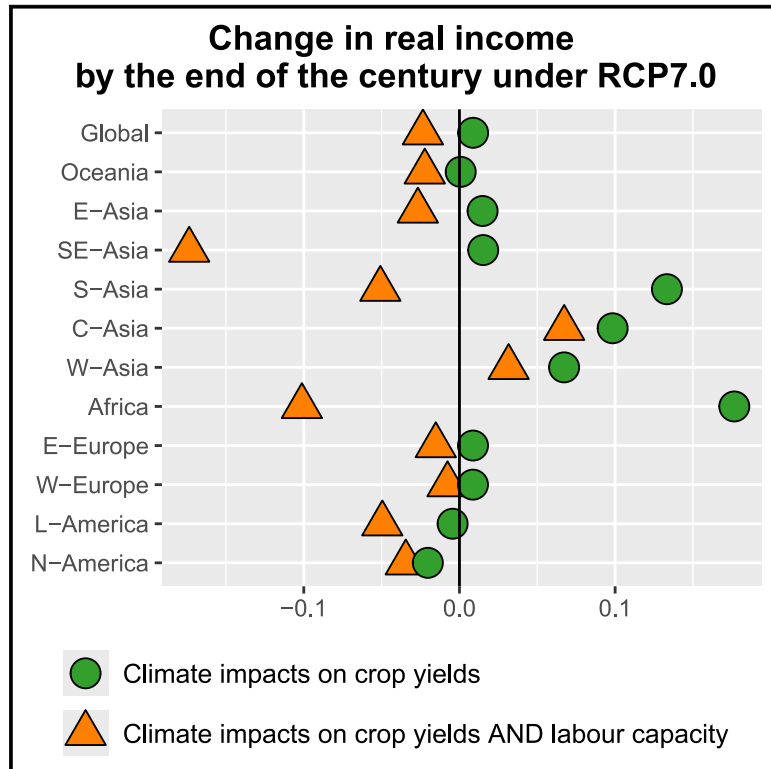


Human heat stress could offset potential economic benefits of CO₂ fertilization in crop production under a high-emissions scenario

Graphical abstract



Authors

Anton Orlov, Jonas Jägermeyr, Christoph Müller, ..., Andrew Smerald, Julia M. Schneider, Jana Sillmann

Correspondence

anton.orlov@cicero.oslo.no

In brief

Climate change can significantly impact agriculture through various channels. Here, we find that climate change will intensify heat stress, resulting in reduced agricultural labor capacity and higher labor costs in Africa and Asia. To mitigate vulnerability to heat stress, proactive adaptation measures, including the deployment of mechanization, are essential.

Highlights

- CO₂ fertilization will lead to higher crop yields under high-emission scenarios
- Thus, crop prices will likely decline under high-emission scenarios
- Heat-stress impacts on labor could substantially increase labor costs
- Heat-stress impacts on labor could outweigh economic benefits of CO₂ fertilization



Article

Human heat stress could offset potential economic benefits of CO₂ fertilization in crop production under a high-emissions scenario

Anton Orlov,^{1,15,*} Jonas Jägermeyr,^{2,3} Christoph Müller,⁴ Anne Sophie Daloz,¹ Florian Zabel,⁵ Sara Minoli,⁴ Wenfeng Liu,^{6,7} Tzu-Shun Lin,⁸ Atul K. Jain,⁹ Christian Folberth,¹⁰ Masashi Okada,¹¹ Benjamin Posch,¹² Andrew Smerald,¹³ Julia M. Schneider,¹⁴ and Jana Sillmann^{1,12}

¹CICERO Center for International Climate Research, Oslo, Norway

²NASA Goddard Institute for Space Studies, New York, NY, USA

³Columbia University, New York, NY, USA

⁴Potsdam Institute for Climate Impact Research, Member of the Leibniz Association, Potsdam, Germany

⁵Department of Environmental Sciences, University of Basel, Basel, Switzerland

⁶State Key Laboratory of Efficient Utilization of Agricultural Water Resources, Beijing, China

⁷Center for Agricultural Water Research in China, College of Water Resources and Civil Engineering, China Agricultural University, Beijing, China

⁸NSF National Center for Atmospheric Research, Boulder, CO, USA

⁹Department of Climate, Meteorology & Atmospheric Sciences, University of Illinois, Urbana, IL, USA

¹⁰Biodiversity and Natural Resources Program, International Institute for Applied Systems Analysis (IIASA), Laxenburg, Austria

¹¹Center for Climate Change Adaptation, National Institute for Environmental Studies, Tsukuba, Japan

¹²Research Unit Sustainability and Climate Risk, Center for Earth System Research and Sustainability (CEN), Universität Hamburg, Hamburg, Germany

¹³Institute of Meteorology and Climate Research, Atmospheric Environmental Research, Karlsruhe Institute of Technology, Garmisch-Partenkirchen, Karlsruhe, Germany

¹⁴Department of Geography, Ludwig-Maximilians-Universität München, Munich, Germany

¹⁵Lead contact

*Correspondence: anton.orlov@cicero.oslo.no

<https://doi.org/10.1016/j.oneear.2024.06.012>

SCIENCE FOR SOCIETY Climate change can significantly affect food production in many ways. Changes in greenhouse gases, temperature, and rainfall directly influence crop productivity, sometimes increasing yield through a mechanism known as the carbon dioxide fertilization effect. However, agricultural production in many countries also relies on physically demanding manual labor, primarily outside, and, as temperatures rise, heat stress on agricultural workers can reduce labor capacity. Consequential climate change impacts on food availability and affordability are a major societal concern, yet the specific and combined impacts on agricultural production remain highly uncertain. An assessment of the future impacts of climate change on the production and prices of four of the world's most consumed crops (maize, wheat, soybean, and rice) reveals that a rise in heat stress will lower agricultural labor capacity and increase labor costs in Africa and Asia. This could offset the potential economic benefits of higher yields due to elevated levels of CO₂. Proactive adaptation measures, such as mechanization deployment, are needed to reduce the vulnerability to heat stress.

SUMMARY

Climate change can significantly impact agriculture, leading to food security challenges. Most previous studies have investigated the direct climate impact on crops while neglecting the impact of heat stress on agricultural labor. Here, we assess the economic consequences of climate impacts on four major crops—maize, soybean, wheat, and rice—for scenarios involving low and high greenhouse gas emissions. Our analysis is based on the output from a new generation of global climate and crop models to drive a multiregional economic model. We find that, even under a high-emission scenario, the effect of CO₂ fertilization could lead to higher yields, resulting in lower prices for major crops, except for maize. However, heat-induced losses in agricultural labor could offset the potential economic benefits of CO₂ fertilization in crop production in Asia and Africa. Our findings emphasize the importance of addressing heat-stress impacts on agricultural labor through proactive adaptation measures.



INTRODUCTION

Under scenarios of high greenhouse gas (GHG) emissions, climate change leads to increasing global temperatures and significant changes in precipitation patterns across regions.¹ Agriculture is especially exposed to climate risks, but, despite recent advances in climate and crop modeling, the climate-induced impacts on agricultural productivity remain highly uncertain.^{2,3} The sensitivities of crop models to key drivers of crop yields—such as carbon dioxide, temperature, water, and nitrogen—vary significantly across different crop models.⁴ On the one hand, an elevated atmospheric concentration of CO₂ will enhance the productivity of many C₃ crops, including wheat, rice, and soybean, through the CO₂ fertilization effect.⁵ At high latitudes, some regions could also experience diminishing temperature limitations (i.e., longer growing seasons) and higher yields due to global warming.⁶ On the other hand, crop yields are expected to decline in regions where critical temperature thresholds are already exceeded. This applies especially to C₄ crops (i.e., carbon is fixed initially into a four-carbon compound during photosynthesis, rendering its assimilation more efficient). Maize, a typical C₄ crop adapted to drier climates, assimilates CO₂ more effectively than C₃ crops but benefits little from an increase in atmospheric concentration of CO₂. The most recent crop model simulations based on phase 6 of the Coupled Model Intercomparison Project (CMIP6) indicate a high likelihood of increased yields for soy, rice, and particularly wheat by the middle of the century, whereas maize yields are expected to decline.³ In addition, the newest scientific evidence shows that climate change will most likely affect crop productivity sooner and more strongly than previously estimated.

Furthermore, apart from direct climate-induced impacts on agriculture (i.e., due to changes in temperature and precipitation), climate change could also indirectly affect agricultural production through climate-induced impacts on capacity and productivity of labor. Agriculture is one of the most labor-intensive sectors, where most physical work is done outdoors and thus is strongly exposed to heat stress.⁷ Under high-warming scenarios, heat stress could significantly reduce labor capacity, especially in the tropics.^{8,9} More frequent and severe humid heat could increase health risks and reduce the capacity for physical work.^{10–12} While shifting working hours could potentially reduce the heat-induced loss of labor productivity under current climatic conditions, this adaptation option will become less effective under future high-warming scenarios as both daytime and nighttime temperatures increase.¹³ Several economic studies showed that the global cost of heat-stress impacts on labor could be considerable.^{14,15} Recent studies also indicate that heat-stress impacts on agricultural labor could lead to a non-negligible global welfare loss.^{16,17} Heat-stress impacts on labor could differ substantially across regions due to different levels of mechanization deployment, with less mechanized regions being most adversely affected by high temperatures.¹⁸

Since crops are tradable goods, regions could be indirectly affected through changes in international prices of crops and processed food products. Hence, not only the direct climatic impacts on crop yields but also the trade position and integration into international crop and food markets will be important factors determining food availability and security.^{19–21} Consequently,

economic responses to climate impacts on crop productivity might not necessarily correspond to the direct climate-induced impacts on yields in a region due to cross-regional and cross-sectoral economic dependencies.

Here we assess the economic consequences of climate impacts on crop yields for four major crops (i.e., maize, wheat, soybean, rice) and heat-stress impacts on labor under low and high GHG-concentration scenarios (i.e., Representative Concentration Pathways [RCPs] 2.6 and 7.0). The biophysical impacts on labor and crop yields are derived from the latest global climate model simulations available from CMIP6²² and crop model simulations available from phase 3 of the Global Gridded Crop Model Intercomparison (GGCMI3).³ Our economic analysis is conducted using the macro-economic model GRACE (Global Responses to Anthropogenic Changes in the Environment),²³ which is a multiregional, multisectoral, computable general equilibrium (CGE). The modeling framework of GRACE can consistently capture cross-regional and cross-sectoral dependencies. We use a static version of GRACE that assesses economic impacts relative to the state of the world economy in 2011. We found that adverse heat-stress impacts on agricultural labor capacity could substantially increase the production cost in Africa and Asia under the high-emission scenario by the end of the century, thereby offsetting a potential economic benefit of the CO₂ fertilization. Proactive adaptation measures in the agricultural sector, such as mechanization deployment, are needed to reduce the vulnerability to heat stress.

RESULTS

Climate impacts on crop productivity

Using GGCMI3 model output, we calculated the regionally aggregated changes in future crop yields relative to the average yields in a historical reference period (1981–2010) for CMIP6's SSP1-RCP2.6 and SSP3-RCP7.0 scenarios (hereafter RCP2.6 and RCP7.0; see “[experimental procedures](#)” section). Thereafter, the projected changes in all four crops were simultaneously implemented in the economic model GRACE to assess the associated impacts on production, food prices, and income by the middle and end of the century relative to the state of the world economy in 2011. [Figure 1](#) compares the yield response, which is derived from GGCMI3 crop model simulations, and the production response, which is the output of GRACE including the market effects. The results of our economic analysis are presented and discussed below. The uncertainty of economic responses, which is represented by error bars in the boxplots, is attributed to a combination of different climate and crop model simulations.

Maize

Most of the crop model simulations show consistent reductions in maize yields in the most important producer regions, especially under the high-emission pathway. Under RCP7.0, the global median reduction in maize yields across the crop model simulations accounts for 8.4% by the end of the century relative to the average yield of 1981–2010 ([Figure 1A](#)). Climate impacts on maize yields differ considerably by region and water management system (i.e., rainfed and fully irrigated) ([Figure S1A](#)). Adverse climate impacts on maize yields can largely be

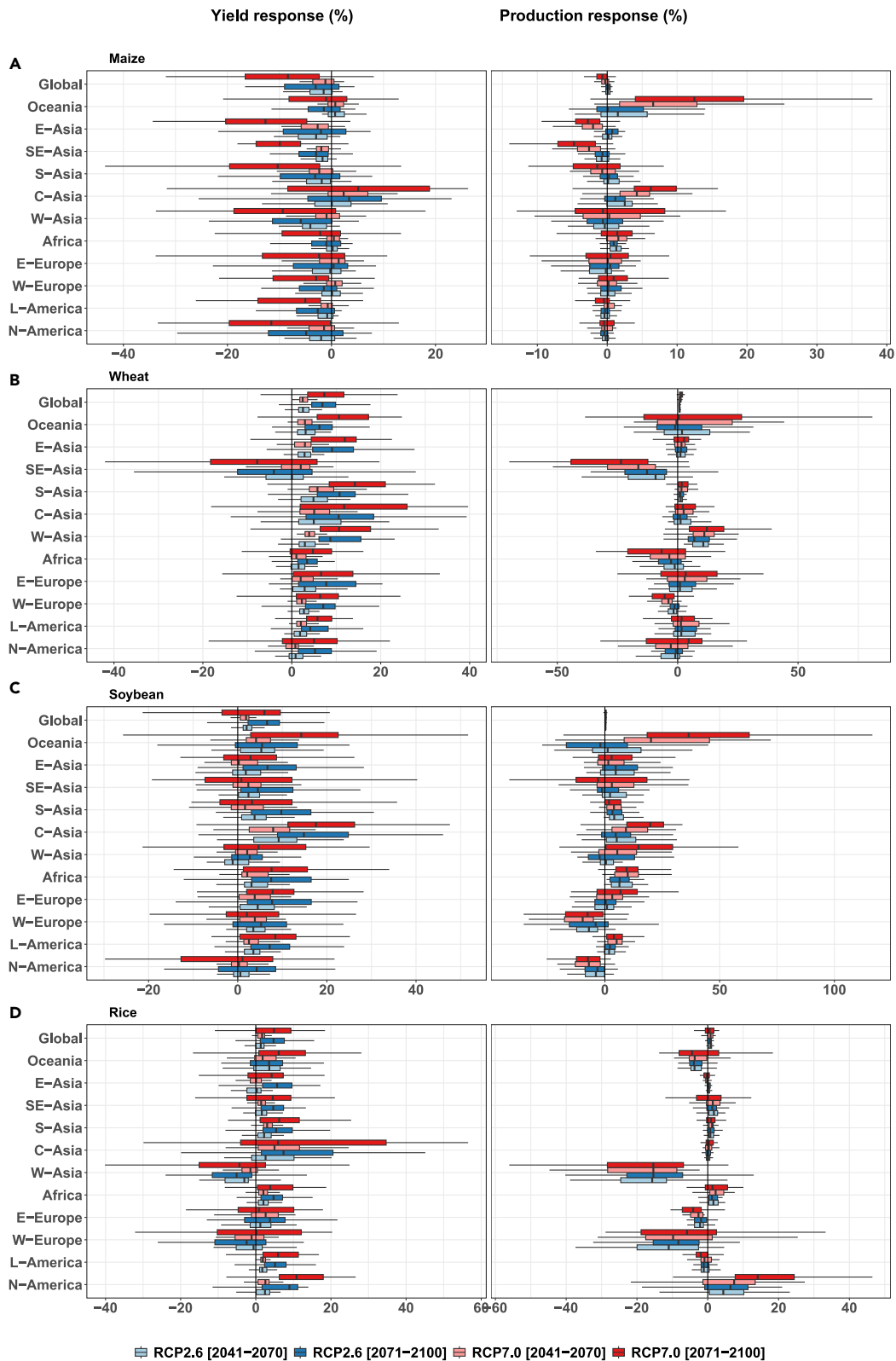


Figure 1. Changes in crop yields and production

Multi-year mean changes in crop yields (left column) and production (right column) of maize (A), wheat (B), soybean (C), and rice (D) by the mid (2041–2070) and end of the century (2071–2100) under RCP2.6 (blue) and RCP7.0 (red) relative to the historical time period (in percent). Yield response is calculated using the

(legend continued on next page)

explained by accelerated phenological development, which includes shorter grain-filling periods, more intense and frequent drought, and a low sensitivity to the CO₂ fertilization effect (see Jägermeyr et al.³ for details). In contrast to C₃ crops, maize as a C₄ plant does not experience a direct stimulation of photosynthesis under an elevated CO₂ concentration. Thus, even under RCP2.6, maize yields are projected to decline in most regions. Furthermore, maize is grown across a wider range of low latitudes, where additional warming could reach critical temperature thresholds by the middle of the century even under RCP2.6.

For most of the crop model simulations, results of the economic model GRACE show a robust decline in global production of maize by the end of the century under both RCPs, especially under RCP7.0, relative to the state of the world economy in 2011 (Figure 2A). The reduction in global production of maize is explained by a lower production in the world's largest maize-producing regions, such as North America (mostly USA) and East Asia (mostly China). For East Asia, the difference in production responses between RCP7.0 and RCP2.6 is more pronounced than for North America. This is because East Asia is located at low latitudes and is therefore more exposed to additional warming. Additionally, South-East Asia experiences a decline in maize production under RCP7.0 for most of the climate-crop model combinations. Under both RCP scenarios, a lower production of maize is associated with higher consumer prices, especially by the end of the century under RCP7.0 (Figure 2A). At the same time, the less adversely affected regions, such as Oceania (mostly Australia) and Central Asia, could experience an increase in maize production, which potentially diminishes the price increase in Oceania and Central Asia. Specifically, Oceania shows a relatively strong increase in production due to an expansion of maize area, since a global increase in maize prices makes it more profitable to grow maize in Oceania. As imported and domestically produced crops are assumed to be imperfect substitutes in consumption, relative changes in the consumer prices of maize differ by region, depending on the biophysical yield response and trade position (i.e., net importer or exporter). For example, Oceania, where most of consumed maize is produced domestically (Figure S2A), shows a smaller increase in the consumer price of maize compared to many other regions. Similarly, Central Asia can even experience a reduction in the consumer price of maize under both RCPs because of increased domestic production.

Wheat

In contrast to maize, wheat yields are simulated to increase at the global level under both RCP scenarios for most of the crop model simulations (Figure 1B). Higher wheat yields can largely be attributed to a strong sensitivity to the CO₂ fertilization effect.³ Moreover, wheat is generally cultivated at higher latitudes, where additional warming is often less harmful or can even lead to yield increases, as is expected to occur in currently temperature-limited regions. Also, results of the crop model simulations show that an increase in yields of rainfed wheat is substantially

larger than for fully irrigated wheat because the CO₂ fertilization effect is strongest under water-limited conditions (Figure S1B).

As a result, for most of the climate-crop model combinations, the GRACE model simulations show a consistent increase in global production of wheat under both RCP scenarios, driven by a higher production in East Asia, South Asia, West Asia, Oceania, and Eastern Europe (Figure 2B). Under RCP7.0, the increase in global production of wheat tends to be higher than under RCP2.6 due to a substantially higher atmospheric CO₂ concentration. For most of the crop model simulations, North America, Western Europe, and Africa experience less pronounced increases in wheat yields compared to many other regions, which could result in a decline in wheat production as it becomes less profitable in these regions. Furthermore, wheat production will likely decline in South-East Asia due to a decline in wheat productivity, although, for South-East Asia, domestic consumption of wheat is satisfied mainly through imports, and changes in domestic production therefore do not have a substantial impact on the consumer price in South-East Asia. For most of the crop model simulations for both RCPs, the regional consumer prices of wheat are projected to decline due to increased yields (Figure 2B). However, under RCP7.0, when driven by climate models with a high equilibrium climate sensitivity (ECS) (i.e., UKESM1-0-LL; see Table 1), some crop models simulate reductions in wheat yields (see low-end whiskers in Figure 1B), and thus the GRACE model simulations point to a possible increase in the regional consumer prices of wheat.

Soybean

Under RCP2.6, results of the crop model simulations also show a relatively robust increase in soybean yields in most regions (Figures 1C and S1C), due mainly to the CO₂ fertilization effect.³ For RCP7.0 compared to RCP2.6, the yield responses are more uncertain, with a wide range of results across climate-crop model combinations, but the median responses of regional yield changes tend to be positive. However, despite relatively strong climate-induced impacts on soybean yields, results of the economic analysis using GRACE show a moderately small impact on global production of soybean (Figure 2C). This is because a higher production in Latin America (mostly Brazil and Argentina) and East Asia (mostly China) is associated with a lower production in another large soybean-producing region, namely North America (mostly USA). An increase in soybean yields in Latin America is stronger than in North America, which induces a reallocation of soybean production from North to South America. Despite potential yield increases, Western Europe will most likely experience a reduction in its domestic production of soybean. However, European production of soybean is modest, and Europe is a net importer of soybean from Brazil and USA. For most of the crop model simulations, soybean production in other regions, especially Oceania, will increase by the end of the century relative to the state of the world economy in 2011. Overall, the regional consumer prices of soybean will most likely decline because of higher yields, and the price responses are similar

GGCM13 crop model ensemble and corresponds to the harvested-area-weighted average of irrigated and rainfed crops. "Production response" is calculated by the GRACE model considering market effects relative to the state of the world economy in 2011. GRACE simultaneously implements yield shocks for all four crops. Heat-stress impacts on labor are not included. The boxes show the interquartile range across climate and crop model ensembles. The whiskers show the variability outside the first and third quantiles, and outliers are removed.

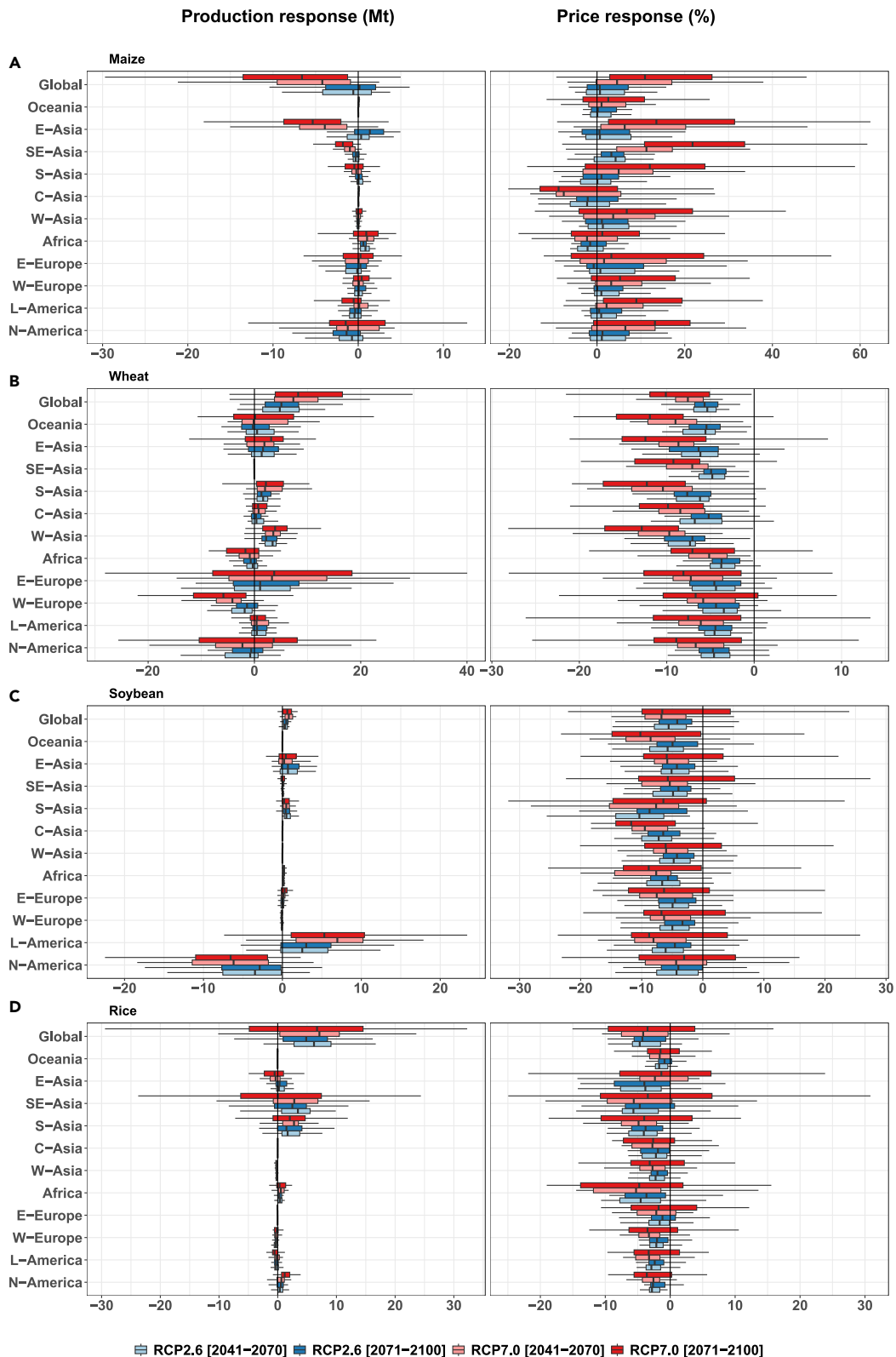


Figure 2. Changes in crop production and prices

Multi-year mean changes in absolute crop production (left column) and consumer prices (right column) of maize (A), wheat (B), soybean (C), and rice (D) by the mid (2041–2070) and end of the century (2071–2100) under RCP2.6 (blue) and RCP7.0 (red) relative to the state of the world economy in 2011. GRACE simultaneously

(legend continued on next page)

Table 1. Overview of scenarios and models

GHG emission scenarios	Climate models	Crop models	Heat-labor exposure-response functions	Economic model
SSP1-RCP2.6	GFDL-ESM4 (ECS: 2.6)	LPJmL	NIOSH	GRACE
SSP3-RCP7.0	MPI-ESM1-2-HR (ECS: 3.0)	PEPIC	Hothaps	
	MRI-ESM2-0 (ECS: 3.2)	CROVER	Laboratory	
	IPSL-CM6A-LR (ECS: 4.6)	EPIC-IIASA		
	UKESM1-0-LL (ECS: 5.3)	ISAM		
		LandscapeDNDC		
		PROMET		

ECS stands for the equilibrium climate sensitivity, which determines a long-term temperature increase in response to a doubling of the atmospheric CO₂ concentration.

across most regions (Figure 2C). Despite a reduction in domestic production, North America also experiences a reduction in the consumer price of soybean under both RCPs, which is associated with an increased import demand for less expensive soybean from Latin America. While the change in global production of soybean is substantially less pronounced than for wheat, the price response is relatively similar. This is because GRACE assumes a less elastic demand for soybean compared to wheat.

Rice

Similar to soybean, under RCP2.6, results of the crop model simulations show relatively consistent increases in rice yields in the largest rice-producing regions, while, under RCP7.0, the yield responses are more uncertain (Figures 1D and S1D). The CO₂ fertilization effect is also the main driver behind an increase in rice productivity. The yield increases of rainfed rice tend to be larger than for fully irrigated rice (Figure S1D). For most of the crop-model combinations, results of the economic analysis using GRACE show a relatively consistent increase in the global production of rice under RCP2.6, which results from a higher production in South and South-East Asia (Figure 2D). For RCP7.0 compared to RCP2.6, relative changes in the global production of rice are more uncertain, especially by the end of the century. Specifically, the future production response of rice in South-East Asia, one of the world's largest rice-producing regions, is highly uncertain under RCP7.0. In contrast to other regions, West Asia experiences a consistent reduction in productivity and production of rice under both RCPs. For most of the climate-crop model combinations, the economic model shows a decline in the regional consumer prices of rice, which is driven by a higher productivity of rice in the world's largest producer regions (Figure 2D).

Food prices and income

Climate-induced impacts on production and prices of unprocessed crops affect the production cost of food products and the income of farmers. In the following, we present and discuss the impact on the food price index and real income (see section "experimental procedures" for definitions). Overall, the results of the economic analysis using GRACE show that the climate-induced impacts on food prices and income are moderately small for most of the crop model simulations relative to the state

of the world economy in 2011. For example, the interquartile range (IQR) of changes in the food price index by the end of the century relative to the baseline does not exceed 2.5%, and, for real income, does not exceed 0.5% (Figure 3). The modest responses of food prices and income are explained by (1) market mechanisms, (2) shares of crops in total production costs of food products, and (3) shares of food products in total consumption expenditure. The first implies substitution possibilities in consumption of imported and domestically produced crops and food products, meaning that, to some extent, trade smooths out the responses of food prices across regions. Regarding the cost composition, according to version 9 of the Global Trade Analysis Project (GTAP9) database²⁴ used in the economic analysis, the share of all crops in the total production cost of primary livestock varies across regions from approximately 5% to 22%, and for processed food products ranges from 6% to 31%, while the remaining cost is attributed to the use of other intermediates and value added (Figure S3). In economically developed regions, the income responses are relatively small because the shares of food products in total consumption expenditures are smaller than in developing regions. Regarding the region-specific impacts, results of the GRACE simulations show that, under RCP2.6, most regions, and especially African and Asian regions, will most likely experience a moderately small decrease in food prices and an increase in real income (Figure 3). For RCP7.0 compared to RCP2.6, the economic impacts are more uncertain, especially by the end of the century (e.g., in South-East Asia) but are still likely to be beneficial in terms of lower food prices and higher real income. The strong adverse impacts on food prices and income are associated with a combination of climate models with a high ECS (i.e., UKESM1-0-LL; see Table 1) and some pessimistic crop models. Regarding the uncertainty decomposition for the end-century global income response, the analysis of variance (ANOVA) shows that, for RCP2.6 (RCP7.0), around 66% (40%) of variance explained is attributed to uncertainty related to general circulation models (GCMs), and for crop model simulations it is 19% (47%) (Figure S4).

Heat-stress impacts on labor

Above, we discussed the economic consequences of direct climate-induced impacts on the productivity of four major crops,

implements yield shocks for all four crops. The production response is measured in million tonnes (Mt). Heat-stress impacts on labor are not included. The boxes show the interquartile range across climate and crop model ensembles. The whiskers show the variability outside the first and third quantiles, and outliers are removed.

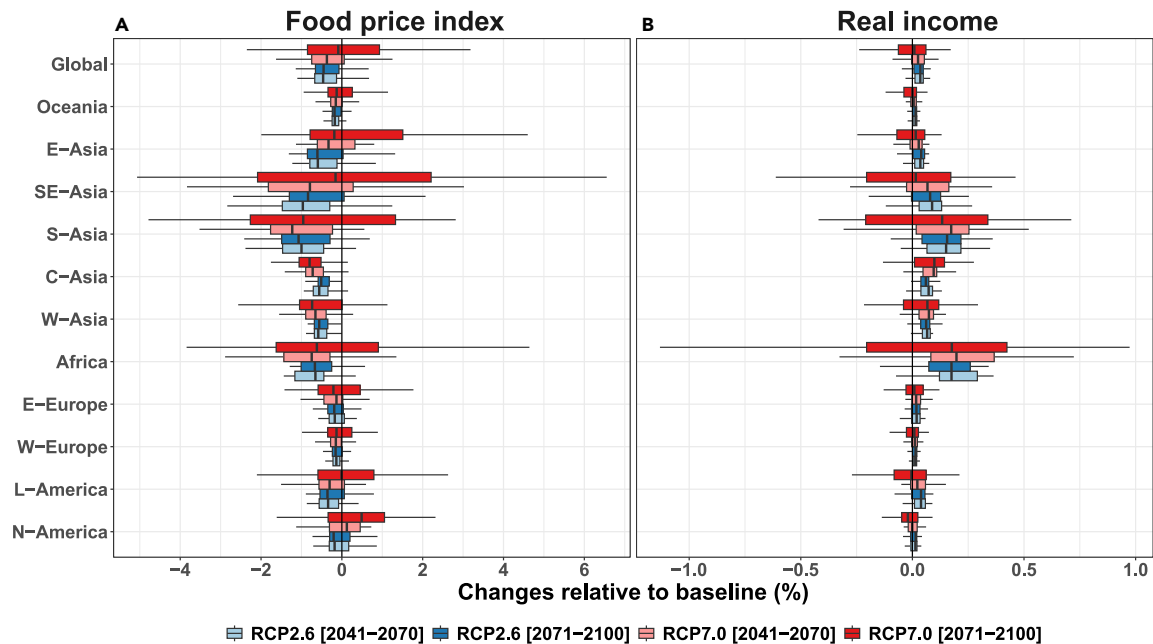


Figure 3. Changes in the food price index and real income

Multi-year mean changes in the food price index (A) and real income (B) by the mid (2041–2070) and end of the century (2071–2100) under RCP2.6 (blue) and RCP7.0 (red) relative to the state of the world economy in 2011. The price and income responses are driven by climate-related crop yield changes without considering heat-stress impacts on labor. The boxes show the interquartile range across climate and crop model ensembles. The whiskers show the variability outside the first and third quartiles, outliers are removed.

driven by changes in temperature, precipitation, and CO₂ concentration. However, agricultural production could also be indirectly affected through human heat-stress impacts. To prevent heat-induced illness, workers should take more frequent and longer breaks, which reduces total work hours. Furthermore, when working under hot weather conditions, heat stress can reduce labor productivity. Heat-induced losses in labor capacity make crop production more expensive because farmers need to hire more workers and/or purchase machinery (e.g., air-conditioned tractors) to cope with a reduced labor capacity. Using the gridded data on temperature, relative humidity, and solar radiation from CMIP6 climate model simulations and heat-labor exposure-response functions, we calculated the heat-induced loss in labor capacity for RCP2.6 and RCP7.0 scenarios (see “experimental procedures” section). The projected losses in labor capacity were implemented in GRACE. In the following, we present the economic responses when the heat-stress impacts on agricultural labor are considered in addition to direct climate-induced impacts on crop yields.

In all the explored scenarios, heat stress is shown to reduce labor capacity, with the impacts being especially strong for South and South-East Asia (Figure S5). Introducing the heat-stress impacts on labor capacity results in higher consumer prices of crops by the middle and end of the century compared to the scenario considering the yield responses alone. While, under RCP2.6, crop prices show only moderately small increases, under RCP7.0 the prices are substantially higher, especially by the end of the century (Figure 4). Heat-stress impacts on labor particularly exacerbate the price increases for maize and significantly diminish the price decreases for soybean and rice. The in-

crease in consumer price of maize is especially strong in South and South-East Asia. For soybean, the price responses in Asia and Africa are more pronounced by the end of the century compared to the middle of the century under RCP7.0 relative to the state of the world economy in 2011, since the heat-stress impacts become more severe. For South Asia, heat-stress impacts on labor turn a decrease in the consumer price of soybean into an increase. For rice, the heat-stress impacts on labor turn a price decrease into a price increase in East and South-East Asia. The price responses of rice to heat-stress impacts on labor are relatively strong compared to other crops because rice is mainly grown in Asian countries, which are at high risk of exposure to heat stress under high-warming scenarios. For wheat, heat-stress impacts on labor do not substantially affect the consumer prices, since wheat is grown across a wide range of high latitudes that are less exposed to heat stress.

As a result of heat-induced losses in labor capacity in production of four major crops, food prices increase in all regions relative to the price levels when only climate change-induced yield responses are implemented. Under RCP2.6, for most regions except South and South-East Asia, the responses of labor capacity have a moderately small effect on food prices and real income by the middle and end of the century (Figure 5). In South-East Asia, even under RCP2.6, heat-induced losses in labor capacity have a relatively strong impact on food prices and real income. East and South Asia, and especially South-East Asia, show large shares of rice in total expenditures on crop consumption (Figure S6), and the income response is thus especially sensitive to changes in rice prices in these regions. Under RCP7.0, the impacts on food prices become substantially

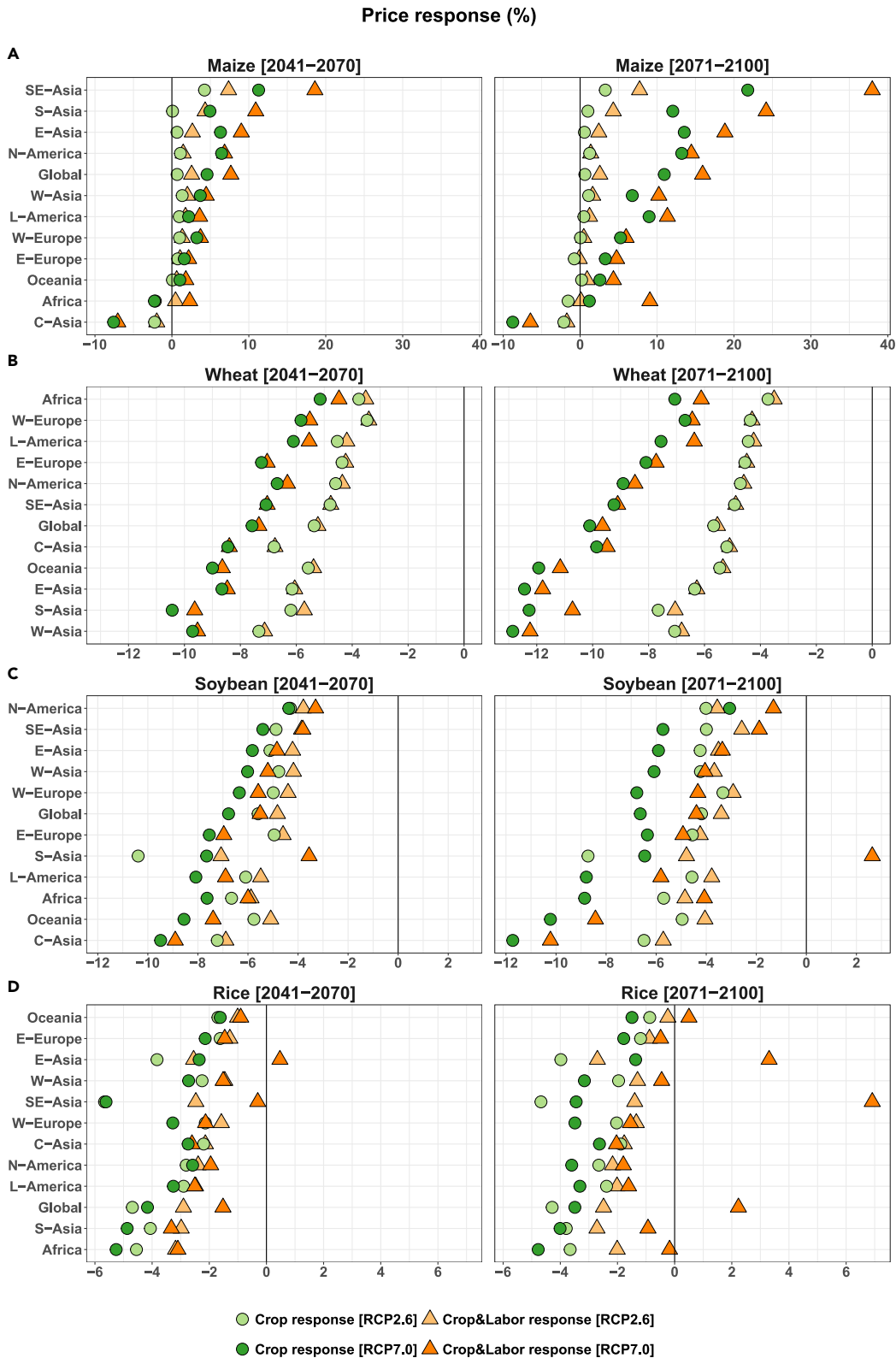


Figure 4. Changes in consumer prices for crops

Median responses of consumer prices for maize (A), wheat (B), soybean (C), and rice (D) by the mid (2041–2070) and end (2071–2100) of the century under RCP2.6 and RCP7.0 relative to the historical time period. The price responses are simulated using the GRACE model and show the median changes over GCMs, crop

(legend continued on next page)

more pronounced, especially by the end of the century. For example, under RCP7.0, almost all regions will likely experience an increase in food prices (Figure 5). Overall, the response of real income corresponds to the response of food price, since an increase in food prices results in a decline in real income. By the end of the century, real income declines in most regions under RCP7.0. For high-latitude regions, heat-induced losses in labor capacity are moderately small, as are the impacts on real income, whereas African and Asian countries experience significantly stronger reductions in real income. Reductions in real income are especially pronounced when using output from climate models with a high ECS (Figure S7). In low-income countries, where wages are the main income source, and food expenditures account for a substantial portion of total income, real wages can be a more direct measure of welfare changes. As shown in Figure 5, the impacts on real wages are substantially more pronounced than those on real income.

The ANOVA shows that, for the end-century global income response under RCP2.6 (RCP7.0), the GCM-related uncertainty attributes around 72% (50%) of variance explained, for crop model simulations it is 15% (38%), and for the heat-labor exposure-response functions it is 0.4% (0.9%) (Figure S4).

Heat-stress impacts also affect the distribution of income between rural and urban households across regions through market mechanisms. Results from the GRACE simulations show that heat-stress impacts on labor could result in an increase in the rural-urban income ratio (see section “[experimental procedures](#)” for definition), which means a reduction in the income gap between rural and urban households (Figure S8). This is because a widespread (global) decline in labor capacity leads to higher crop prices. As the price elasticities of demand for food products are relatively low, the positive effect of increased crop prices tends to be stronger than the negative effect of a reduction in demand and production.²⁵ To compensate for the heat-induced loss in labor capacity, the demand for agricultural labor increases relative to the historical time period (i.e., no further climate change), thereby leading to higher wages. Thus, an increase in crop prices is absorbed by an increase in rural income. Results of the GRACE simulations show that a higher demand for labor due to heat-induced losses in labor capacity is associated with a relocation of labor from non-agriculture to agriculture in many regions. A negative correlation between agricultural productivity and labor demand was also founded in an empirical study from Liu et al.²⁶

Beyond the major crops

Above, we evaluated the economic responses of climate impacts on only four major crops (i.e., maize, wheat, soybean, and rice). However, other crops are also an important source of nutrition and income in many countries. In particular, vegetables and fruit, whose production is also labor intensive, account for a large share of total consumption expenditures as well as a large share of value added in the gross domestic product (GDP) in African and Asian countries (Figure S6). In an additional simulation using GRACE, we introduce the heat-stress impacts on la-

bor capacity in production of all types of crops, including grains, vegetables, and fruits in addition to four major crops. Due to a lack of data, following Müller and Robertson,²⁷ we assume that the yield responses of other crops equal the average yield response of three major C₃ major crops (i.e., wheat, soybean, rice). We found that, when implementing the climate-induced impacts on all types of crops, the decreases in food prices and the increases in real income are larger compared to those when only productivity of four major crops is affected by climate change. This is because the CO₂ fertilization effect results in higher productivity and, therefore, lower consumer prices of other crops (i.e., vegetables and fruit) (Figure S9). However, the heat-induced losses in labor capacity diminish the decreases in food prices, especially in Asia and Africa (Figure S10). This emphasizes that the adverse heat-stress impacts on agricultural labor could have a non-negligible impact on the welfare of households in the most vulnerable low-latitude, low-income regions under high-warming scenarios.

While the modeling framework of GRACE endogenously depicts the mechanization of crop production through substitution between labor, land, and capital, results from the GRACE simulations show that, due to budget constraints, many farmers cannot afford to fully mechanize crop production. In an additional sensitivity experiment, we implement more proactive mechanization at no cost by assuming that work intensity in crop production is equivalent to an average work intensity in the service sector, which implies a low intensity of physical work (see section “[climate labor shifters](#)”). Results of this sensitivity experiment show that such a radical mechanization of crop production would significantly reduce the adverse heat-stress impacts on food prices and income (Figure S10). However, a more proactive mechanization deployment would also require massive investment costs and government support, which could be financially infeasible in poor regions due to fiscal constraints.

DISCUSSION

The separate and combined climate-induced impacts on agriculture are highly uncertain. Most previous studies have primarily focused on the direct climate impact on crop yields, while neglecting the effects of human heat stress on agricultural labor. Here we assess the economic consequences of future climate-related impacts on the production and prices of four major crops under both low- and high-emissions scenarios. Our economic analysis uses the latest crop model simulations, based on CMIP6. These simulations reveal significantly greater crop yield responses to climate change compared to previous ones based on CMIP5.³ The results of our economic analysis show no robust evidence of welfare losses due to climate change-induced impacts on crop productivity. This contradicts the findings of some previous global economic studies based on a meta-analysis compiled for the Intergovernmental Panel on Climate Change (IPCC) 5th Assessment Report.^{16,28,29} While maize productivity will most likely decline in most regions even under a low-emission scenario, crop model simulations indicate a high

models, and heat-labor ERFs. The circles in shades of green labeled “Crop response” show the scenarios that only consider the climate-related yield responses of the four crops. The triangles in shades of orange labeled “Crop&Labor response” show the scenarios that consider both yield changes and heat-stress impacts on labor of the four crops.

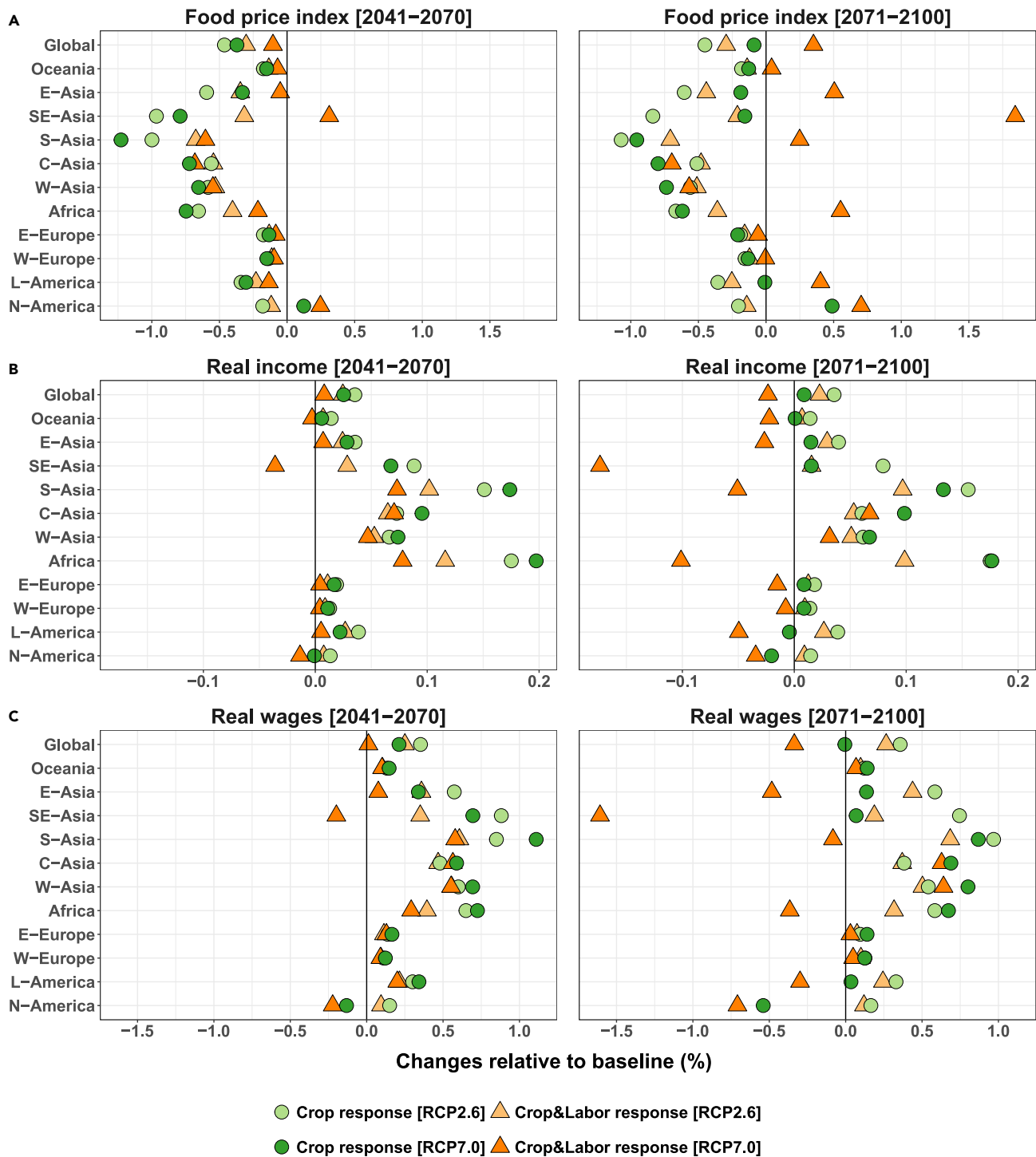


Figure 5. Changes in the food price index, income, and wages

Median responses of the food price index (A) and regional real income (B) and real wages (C) by the mid (2040–2070) and end (2071–2100) of the century under RCP2.6 (green) and RCP7.0 (orange) relative to the historical time period. The income and price responses are simulated using the GRACE model and show the median changes across GCMs, crop models, and heat-labor ERFs. The circles in shades of green labeled “Crop response” show the scenarios that only consider the climate-related yield responses of the four crops. The triangles in shades of orange labeled “Crop&Labor response” show the scenarios that consider both yield changes and heat-stress impacts on labor of the four crops.

probability of an increase in yields of wheat, soybean, and rice even under a high-warming scenario. An increase in crop productivity will result in higher production and lower consumer prices. The CO₂ fertilization effect is one of the main reasons for higher crop yields. The primary divergence between our findings and those of previous studies likely comes from the selection of crop models. de Lima et al.¹⁶ and Moore et al.^{28,29} conducted a meta-analysis, incorporating published yield response estimates from various sources to develop climate-yield response functions. Their meta-analysis likely relies on a different ensemble of crop projections, which show significantly more pessimistic outcomes compared to our own. The selection of crop models (ensemble) for projecting yields in response to climate and atmospheric CO₂ changes significantly influences the projected ensemble mean yield response.^{4,30}

Although crops are imperfect substitutes in consumption, the results of our analysis show that the total impact on food prices and household income is moderately small and likely positive in many regions, which is in line with some previous studies.^{17,31} Nevertheless, for climate models with high-end warming levels and more pessimistic crop models, which represent the extreme ends of the distribution, the adverse warming effect could dominate the CO₂ fertilization effect.³² This emphasizes the relevance of uncertainty ranges in climate and crop responses (i.e., different warming and crop yield responses to the same CO₂ concentration). The CO₂ fertilization effect still introduces one of the largest sources of uncertainty for the end-century yield responses under high-emissions scenarios.⁵

Furthermore, we found that human heat stress could have a relatively strong impact on food prices and income compared to the direct climate-induced impact on crop productivity. Crop production, and especially rice production in low-latitude regions with low mechanization, is expected to be most adversely affected by heat stress. While the labor responses to heat stress are modest by the middle of the century under both RCP scenarios, the end-century impacts become substantially more adverse under a high-warming scenario. More proactive adaptation measures, such as mechanization deployment, will be needed to reduce the heat-induced losses of labor capacity in agriculture. However, the cost of adaptation might be larger under a high-emission scenario, especially in a world facing a high level of regional poverty and inequality. We also found that higher prices of crops could reduce the income gap between rural and urban households in some regions, because the positive price effect could be greater than the negative production effect. However, the income response will also depend on farm size, adaptive capacity, and how income is distributed between farm workers and landowners. In regions with high inequality and poor governance, the income could be disproportionately distributed in favor of landowners.^{33,34} Moreover, mainly large farms could benefit from higher crop prices, whereas small farms might not be able to cope with adverse heat-stress impacts. Overall, human heat stress could not only lead to adverse health impacts but could also challenge the implementation of sustainable development goals (SDG) on poverty and food security (i.e., SDG1 and SDG2). Restrictive agricultural trade policies, such as export restrictions on crops, which can be implemented to ensure domestic food security in response to temporal in-

creases in food prices, could aggravate an increase in food prices in importing countries.^{35–37}

This study has some caveats and limitations that need attention in future research. While the mid-century economic impacts are relatively similar between RCP2.6 and RCP7.0, the end-century impacts based on RCP7.0 might be overestimated in our economic analysis. Based on current nationally determined contributions, RCP4.5 and 6.0 appear to be more realistic future scenarios than RCP7.0. However, the latest crop model simulations are available only for RCP2.6, RCP7.0, and RCP8.5. Climate and crop models might underestimate the impacts of climate extremes.^{38,39} The positive yield response due to enhanced CO₂ could also be overestimated because the crop model simulations do not include any impact of ozone changes. In the near term, the adverse ozone effect could be stronger than the CO₂ fertilization effect.⁴⁰ In contrast to crop models, GRACE explicitly implements several adaptation measures, such as irrigation expansion, input substitution in production, and land-use change but at a highly aggregated regional and sectoral scale. In this analysis, we investigate the economic responses to long-term climatic trends, while the impacts of climate extremes (i.e., drought and extreme precipitation) are beyond the scope of this study. In the long term, market mechanisms could smooth and diminish adverse climate impacts on food prices. Nevertheless, the market mechanisms do not apply for remote regions without access to the market. Moreover, in the short term, the market mechanisms and adaptation could be hampered by market imperfection and inertia in the economic system.⁴¹ Climate impacts on the welfare of subsistence farmers are not quantified in our economic analysis. A combination of macro- and micro-economic analyses could give useful insights into potential impacts on poverty and income distribution across different income groups. Furthermore, we investigate only adverse heat-stress impacts on labor, while a warmer climate could lead to a higher labor capacity in high-latitude regions. More empirical research is needed to estimate region- and sector-specific exposure-response functions for climate-related impacts on capacity and productivity of labor. Due to a lack of data, our analysis focuses on the four major crops. Future research should include non-staple crops because these are an important source of nutrition and income.⁴² Climate-induced migration across regions, which could also induce considerable socio-economic effects, is not implemented in the economic model. Our analysis relies on a static version of GRACE, which evaluates economic impacts relative to the state of the global economy in 2011. However, future economic impacts may significantly differ due to socio-economic shifts, particularly technological advancements such as mechanization. In this context, our economic analysis can overestimate the economic cost of heat stress by the end of the century. In future research, this can be tackled by creating sector-specific projections for agricultural production and trade, along with dedicated mechanization pathways.

In our analysis, we use daily mean values of climate variables to quantify the heat-stress indices and labor capacity. This approach does not consider the diurnal cycle of climate variables. To assess the sensitivity of the results to this limitation, we compare labor capacity based on daily mean and disaggregated hourly climate data⁴³ assuming a 7 a.m. to 7 p.m. workday

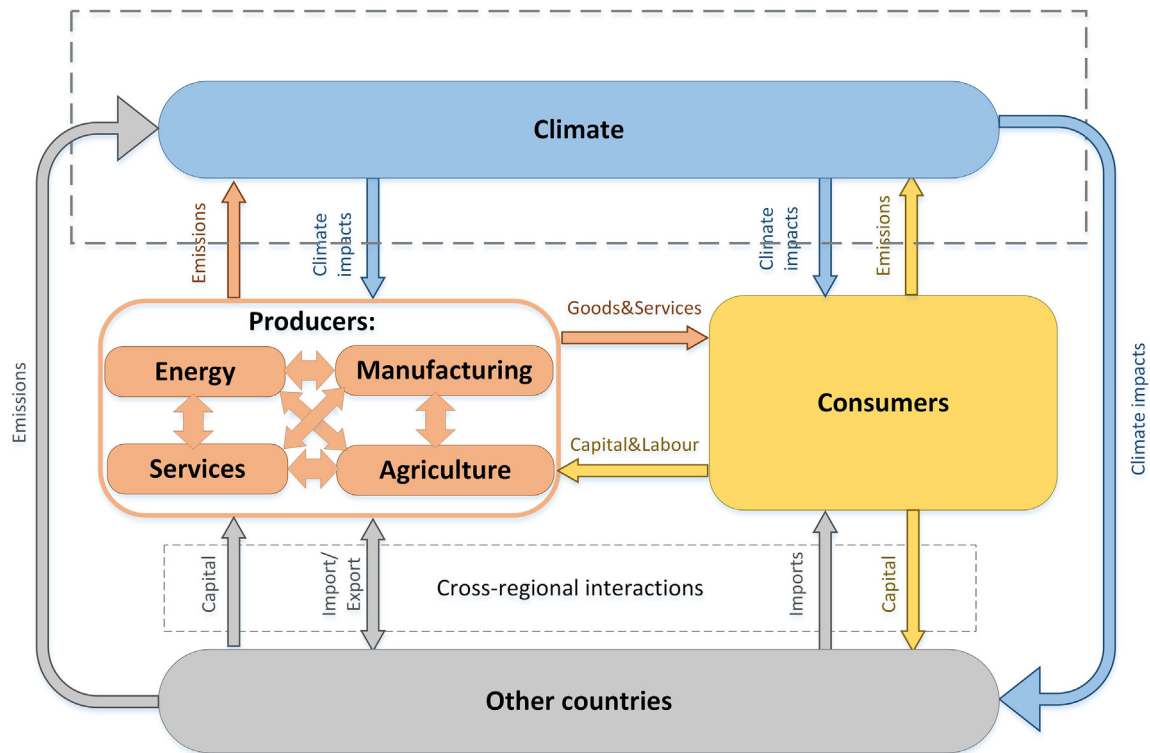


Figure 6. The flowchart of key processes in the GRACE model

Circular flows of economic activities and climate-economic interactions within a region (country) in GRACE. The climate component is not an endogenous part of GRACE's economic optimization. Biophysical climate-induced shocks are derived from climate and impact models and exogenously incorporated into GRACE, meaning that the feedback effects of the economy on climate are not accounted for.

without considering shifts in working hours (see [supplemental information](#)). The comparison is carried out at 30 locations globally, representing major agricultural regions ([Figure S11](#)). We find that using daily mean values leads to an underestimation of the heat-induced impacts on labor capacity. The degree of underestimation varies by location and season, with the largest deviations occurring in the warm seasons in high latitudes ([Figure S12](#)). Despite some limitations, the results of this study emphasize the relevance of human heat stress in agricultural production for food security and highlight the need for more proactive adaptation measures to reduce the health risk and economic costs of heat-stress impacts on agricultural labor.

EXPERIMENTAL PROCEDURES

Resource availability

Lead contact

Further information and requests should be directed to and will be fulfilled by the lead contact, Anton Orlov (anton.orlov@cicero.oslo.no).

Materials availability

This study did not generate new unique materials.

Data and code availability

Data to calibrate the GRACE model were obtained from GTAP9: <https://www.gtap.agecon.purdue.edu>. The code of the GRACE model and simulation results presented and discussed in this study are available upon request. The biased-adjusted daily Inter-Sectoral Impact Model Intercomparison Project (ISIMIP) CMIP6 data for near-surface daily mean temperature and relative humidity are publicly accessible at <https://data.isimip.org/search/tree/>

[ISIMIP3b/InputData/climate/simulation_round/ISIMIP3b/](#). The crop model simulations are publicly accessible at https://www.isimip.org/outputdata/?simulation_round=ISIMIP3b.

Methodology

Economic model

To assess the economic responses to climate impacts on crop yields and labor capacity, we used a standard multiregional and multisectoral CGE model: GRACE.²³ A detailed description of GRACE can be found in Aaheim et al.²³ GRACE describes the economic interactions associated with production, consumption, and trade of commodities, products, and services ([Figure 6](#)) based on the GTAP9 database.²⁴ GTAP9 represents the economic interactions (i.e., production costs, consumption expenditures, and bilateral trade flow) between producers and consumers. GTAP9 data are compiled using regional input-output tables. In the model, producers are assumed to maximize profit subject to resource and technology constraints, and consumers are assumed to maximize welfare (utility) from consumption of goods and services subject to budget constraints. The main economic equilibrium conditions are (1) market clearance (i.e., demand equals supply), (2) zero profit (i.e., production revenue equals production cost), and (3) income balance (i.e., income equals expenditures). In this study, we used a modified version of GRACE with a more sophisticated depiction of the agro-economy,¹⁷ a description of which can also be found in the supplemental experimental procedures. The main agro-economic features implemented in the model are (1) conversion costs of land-use change and (2) an explicit representation of two water management systems (fully irrigated and rainfed). In the model, production of crops could be increased through both land-use change and intensification but constrained by resource availability (i.e., labor, capital, land, and water). In GRACE, the regional production and prices are determined not only by direct climate impacts on yields but also by market mechanisms. The latter are associated with the interaction between demand and supply, and cross-sectoral and

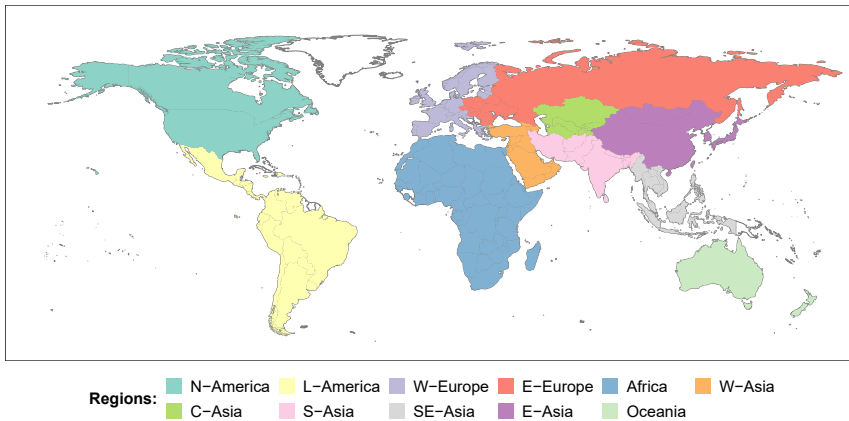


Figure 7. Regional aggregation in GRACE

cross-regional dependencies. Also, the competition for land among different types of crops affects the production patterns. Hence, the market mechanisms might cause non-trivial production and price responses to direct climate impacts. In GRACE, domestically produced commodities are supplied to domestic and export markets. Applying the Armington approach,⁴⁴ which is widely implemented in standard CGE models, domestic and imported commodities are modeled as imperfect substitutes using the constant elasticity of substitution (CES) functions. Imperfect substitutability between imported and domestic crops implies that crops have different characteristics and quality, so consumer prices of crops are region specific (i.e., no single global price). The values of substitution elasticities between imported and domestic commodities are taken from the GTAP database. Since major crops are relatively homogeneous goods, the values of substitution elasticities are higher than for manufactured goods. Furthermore, agricultural and non-agricultural goods are modeled as imperfect substitutes. We assume an imperfect mobility of labor across sectors, which is implemented using a constant elasticity of transformation (CET) function, but labor is immobile across regions (i.e., no migration). Capital is mobile across sectors and regions. The conversion cost of land-use changes is depicted by a nested-CET function. While total land availability is constrained, land use for different types of crops and pasture is endogenously determined in GRACE by market mechanisms. We used a static version of the model, which implies that economic impacts are estimated relative to the reference year of 2011. For our economic analysis, we aggregated the monetary values of consumption expenditures, production costs, and trade flows of all countries presented in the GTAP database into 11 world regions (Figure 7; Table S1). Price responses of wheat, which are simulated by GRACE, were validated against historical data in Zhang et al.⁴⁵ GRACE was also validated through theoretical modeling and sensitivity analyses with respect to key parameters of the model (i.e., substitution elasticities in production and consumption).⁴⁶

Our economic impact assessment was conducted for two GHG emission scenarios: CMIP6's SSP1-RCP2.6 and SSP3-RCP7.0 (hereafter RCP2.6 and RCP7.0, because only climate component is considered in our analysis).⁴⁷ The former implies a strict mitigation policy, which leads to an increase of global annual mean surface temperature below 1.3°C–2.4°C by the end of the century relative to 1850–1900. The latter is associated with a 2.8°C–4.6°C increase of global annual mean surface temperature due to higher GHG emissions.¹ Using GRACE, we conducted two simulations per scenario. First, we incorporated the biophysical crop yield changes derived from the crop model ensemble.⁵ Second, in addition to the climate impacts on crop yields, we introduced the heat-stress impacts on labor capacity.

GRACE quantifies the climate-induced impacts on regional production and consumer prices of crops, food prices, and income. A regional consumer price of crop is calculated as a consumption-weighted price of import and domestic crops. The total impact on food prices is measured by a food price index, which is a consumption-weighted average price of a basket of food products. An increase (decrease) of crop productivity in a region tends to lead to lower (higher) regional food prices. GRACE is a multi-region and multi-sector model that shows the changes in equilibrium prices. Thus, changes in crop produc-

tivity in outermost regions could also affect regional food prices because of trade. The impact on food prices also depends on the trade position (i.e., net exporter vs. importer of crops) as well as demand elasticities for crops and food products. Moreover, the production and price of a crop depend on how other crop types are affected by climate change because of competition for land. Real income is a nominal income deflated by the consumer price index (CPI). Nominal income includes earnings from providing primary production factors such as labor, capital, land, and other natural resources. These earnings are subsequently allocated toward both consumption and savings. For each region, consumers are modeled by a representative household. In our analysis, real income is used as a welfare index because it accounts for both changes in consumer prices and income. We also assess the impact on real wages, which serves as another indicator of welfare. Real wages measure the purchasing power of wages and are computed by taking the economy-wide average wage and adjusting it for inflation using the food price index. Moreover, to analyze potential impacts on income distribution between rural and urban households, based on results from the GRACE simulations, we compute a rural-urban income ratio, which quantifies changes in rural income relative to urban income. Rural income is defined as the weighted average income from the agricultural sector, and urban is the weighted average income from non-agricultural sector. We use the initial shares of income from labor, capital, and land as a weighting factor.

consumers are modeled by a representative household. In our analysis, real income is used as a welfare index because it accounts for both changes in consumer prices and income. We also assess the impact on real wages, which serves as another indicator of welfare. Real wages measure the purchasing power of wages and are computed by taking the economy-wide average wage and adjusting it for inflation using the food price index. Moreover, to analyze potential impacts on income distribution between rural and urban households, based on results from the GRACE simulations, we compute a rural-urban income ratio, which quantifies changes in rural income relative to urban income. Rural income is defined as the weighted average income from the agricultural sector, and urban is the weighted average income from non-agricultural sector. We use the initial shares of income from labor, capital, and land as a weighting factor.

Climate-yield shifters

The projected yield changes of four major crops (i.e., maize, wheat, soybean, and rice) are taken from the GGCMI3 crop model simulation archive.⁴⁸ We used the crop yield simulations from an ensemble of seven crop models, driven by five CMIP6 climate models, which are down-scaled and bias adjusted by ISIMIP (Table 1). Crop model simulations provide crop yields for two water management regimes: rainfed and fully irrigated. Fully irrigated means that there are no water availability constraints for crop irrigation and the models apply as much water as was requested by the plants. While 12 crop models participated in GGCMI3, only seven crop models provided simulations for RCP7.0. We take RCP7.0 as a high-end GHG emissions scenario as RCP8.5 has recently been criticized for being unrealistic.⁴⁹ The ensemble of climate models covers the range of ECS of the full CMIP6 ensemble, with a range of 2.6–5.3.⁵⁰ We used crop model simulations that explicitly consider changing atmospheric CO₂ concentrations depending on the RCP scenario. All crop model simulations implement fixed 2015-year direct human influences (i.e., land use, nitrogen deposition, and fertilizer). The new generation of crop models distinguish between winter and spring wheat, and two rice seasons (i.e., first and second growing period), while the GTAP database used in our analysis provides aggregated annual economic values. Therefore, we calculated the yield responses of wheat and rice using the maximum values of winter and spring wheat and two rice seasons, respectively. Because GRACE is resolved at an aggregated regional scale (Figure 7), we aggregated the spatially explicit data on crop yields at a 0.5° × 0.5° geographic grid resolution to the same regions represented in GRACE using crop-specific harvested area⁵¹ as a weighting factor. Then, the harvested-area-weighted yields were smoothed using the method of rolling averages to obtain long-term trends of climate-induced changes in crop productivity. Finally, for each crop type, water management system (i.e., rainfed and fully irrigated), RCP, and climate and crop model combination, we calculated the changes in crop yields in future scenarios relative to the average yields in a reference period (1981–2010) (hereafter, the climate yield shifters). The climate yield shifters were used in GRACE as scaling factors for total factor productivity of crop production. The climate yield shifters include the crop yield response to changes in both atmospheric CO₂ concentrations and climatic variables (i.e., temperature and precipitation). Note that all crop model simulations isolate the climate

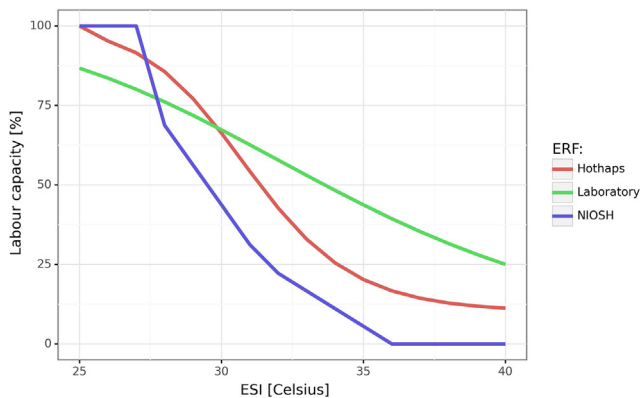


Figure 8. Heat-labor ERFs showing the relationship between labor capacity and environmental stress index (ESI) for high work intensity

signal and do not assume any adaptation measures or changes in management. However, some adaptation measures, such as irrigation; land-use change; mobility of capital and labor; and substitution between capital, labor, and land, are endogenously implemented in GRACE.

Climate labor shifters

The heat-stress impacts on labor capacity were quantified using the wet-bulb global temperature (WBGT) and the environmental stress index (ESI). The WBGT measures a combined effect of temperature and humidity on heat stress in shade (i.e., shielded from the sun), while the ESI also includes the additional effect of solar radiation. Specifically, the WBGT was computed using the biased-adjusted daily ISIMIP CMIP6 data on near-surface daily mean temperature (*tas*) and relative humidity (*hurs*) by applying the empirical model from Stull⁵² (Equations 1 and 2). To calculate the ESI, we applied the empirical model from Moran et al.⁵³ using the data on near-surface daily mean temperature, relative humidity, and surface downwelling shortwave radiation (*rsds*) available from the same CMIP6 climate models used in the crop model simulations (Equation 3). ESI is found to be an accurate approximation for more precise iterative methods to calculate WBGT for outdoors.^{53–55}

$$WBGT_{shade} = 0.67 * WBGT_{stull} + 0.33 * tas \quad (\text{Equation 1})$$

$$WBGT_{stull} = tas * \text{atan}\left(c1 * \sqrt{hurs+c2}\right) + \text{atan}(tas + hurs) - \text{atan}(hurs - c3) + c4 * \left(hurs^{\frac{3}{2}}\right) * \text{atan}(c5 * hurs) - c6 \quad (\text{Equation 2})$$

$$ESI = 0.63 * tas - 0.03 * hurs + 0.002 * rsds + 0.0054 * tas * hurs - \left(\frac{0.073}{0.1+rsds}\right) \quad (\text{Equation 3})$$

Using the WBGT and ESI, labor capacity was computed applying three heat-labor exposure-response functions (ERFs). One is based on field studies, which were synthesized for the “high occupational temperature health and productivity suppression” program (Hothaps).^{56,57} Another one is derived from the National Institute for Occupational Safety and Health (NIOSH) standards.^{58,59} The third is based on an experiment trial where physical work was simulated using treadmill-based walking (hereafter, Laboratory ERF).⁶⁰ For our economic analysis, we used the mean values of labor capacity levels estimated for indoor (WBGT) and outdoor (ESI) work environment, because workers try to avoid full sun exposure by moving some tasks to times when it is less hot. Moreover, in the tropics, ~40% of days are cloudy.⁹ Using three ERFs (i.e., Hothaps, NIOSH, and Laboratory) aims to capture uncertainty ranges of heat-stress impacts on labor (Figure 8). The NIOSH, Hothaps, and Laboratory ERF do not consider any adaptation, but GRACE assumes mobility of capital and labor as well as substitutability between capital and labor (i.e., mechanization). Moreover, shifting working hours is also implicitly included

in our analysis because daily mean values of climate variables are used to compute the heat-induced impacts on labor capacity.

We computed the heat-stress impacts on labor capacity for three levels of work intensity (i.e., high, moderate, and low work intensity). For the core simulations of GRACE, a moderate work intensity in crop production is assumed for North America, Western Europe, Oceania, and Eastern Europe because these regions are relatively mechanized. For all other regions, crop production is assumed to require a high work intensity. For a sensitivity test on more proactive mechanization, we used the estimates for low work intensity, which is equivalent to work intensity in the service sector. The heat-stress impacts on labor were calculated for each RCP and climate model using a similar procedure as for crops: (1) we aggregated the daily heat-stress impacts on labor to annual average values using the crop calendar for GGCM13⁴⁸ as a weighting factor, then (2) aggregated the spatially explicit impacts to 10 world regions represented in GRACE using the harvested area as a weighting factor; (3) we calculated the rolling averages; and finally (4) we computed the changes in labor capacity in future projections relative to the average level of labor capacity in the reference scenario (1981–2010) (hereafter, the climate labor shifters). The climate labor shifters were used in GRACE as the scaling factors for labor productivity in crop production.

SUPPLEMENTAL INFORMATION

Supplemental information can be found online at <https://doi.org/10.1016/j.onear.2024.06.012>.

ACKNOWLEDGMENTS

We want to thank two anonymous referees for their valuable comments, which significantly enhanced the quality of our paper. A.O. and J.S. were funded by the European Union Horizon 2020 project “Remote Climate Effects and their Impact on European Sustainability, Policy and Trade” (RECEIPT) (grant agreement no. 820712). J.S. and B.P. were supported by the German Research Foundation (DFG) under Germany’s Excellence Strategy—EXC 2037: “CLICCS – Climate, Climatic Change, and Society”—project no. 390683824, contribution to the Center for Earth System Research and Sustainability (CEN) of Universität Hamburg. T.-S.L. and A.K.J. were supported by the US NSF (831361857). M.O. was supported by the Environmental Research and Technology Development Fund (JPMEERF20S11805) of the Environmental Restoration and Conservation Agency of Japan. W.L. was supported by the National Natural Science Foundation of China (52109071 and 52239002).

AUTHOR CONTRIBUTIONS

A.O. conducted the analysis and wrote the paper. J.S. and A.S.D. developed the conceptual framing and commented on the manuscript. F.Z. provided the crop model simulations and hourly climate data. B.P. provided the hourly climate data and commented on the manuscript. J.J., C.M., S.M., W.L., T.-S.L., A.K.J., C.F., and M.O. provided the crop model simulations and commented on the manuscript. A.S. and J.M.S. provided the crop model simulations.

DECLARATION OF INTERESTS

The authors declare no competing interests.

Received: November 27, 2023

Revised: April 19, 2024

Accepted: June 21, 2024

Published: July 19, 2024

REFERENCES

1. IPCC (2021). Summary for Policymakers. In *Climate Change 2021: The Physical Science Basis. Contribution of Working Group I to the Sixth Assessment Report of the Intergovernmental Panel on Climate Change*, V. MassonDelmotte, P. Zhai, A. Pirani, S.L. Connors, C. Péan, S. Berger,

- N. Caud, Y. Chen, L. Goldfarb, and M.I. Gomis, eds. (Cambridge University Press).
2. Müller, C., Franke, J., Jägermeyr, J., Ruane, A.C., Elliott, J., Moyer, E., Heinke, J., Falloon, P.D., Folberth, C., Francois, L., et al. (2021). Exploring uncertainties in global crop yield projections in a large ensemble of crop models and CMIP5 and CMIP6 climate scenarios. *Environ. Res. Lett.* *16*, 034040. <https://doi.org/10.1088/1748-9326/abd8fc>.
 3. Jägermeyr, J., Müller, C., Ruane, A.C., Elliott, J., Balkovic, J., Castillo, O., Faye, B., Foster, I., Folberth, C., Franke, J.A., et al. (2021). Climate impacts on global agriculture emerge earlier in new generation of climate and crop models. *Nat. Food* *2*, 873–885. <https://doi.org/10.1038/s43016-021-00400-y>.
 4. Müller, C., Jägermeyr, J., Franke, J.A., Ruane, A.C., Balkovic, J., Ciais, P., Dury, M., Falloon, P., Folberth, C., Hank, T., et al. (2024). Substantial Differences in Crop Yield Sensitivities Between Models Call for Functionality-Based Model Evaluation. *Earth's Future* *12*, e2023EF003773. <https://doi.org/10.1029/2023EF003773>.
 5. Toreti, A., Deryng, D., Tubiello, F.N., Müller, C., Kimball, B.A., Moser, G., Boote, K., Asseng, S., Pugh, T.A.M., Vanuytrecht, E., et al. (2020). Narrowing uncertainties in the effects of elevated CO₂ on crops. *Nat. Food* *1*, 775–782. <https://doi.org/10.1038/s43016-020-00195-4>.
 6. Wiréhn, L. (2018). Nordic agriculture under climate change: A systematic review of challenges, opportunities and adaptation strategies for crop production. *Land Use Pol.* *77*, 63–74. <https://doi.org/10.1016/j.landusepol.2018.04.059>.
 7. Poulianiti, K.P., Havenith, G., and Flouris, A.D. (2019). Metabolic energy cost of workers in agriculture, construction, manufacturing, tourism, and transportation industries. *Ind. Health* *57*, 283–305. <https://doi.org/10.2486/indhealth.2018-0075>.
 8. Dunne, J.P., Stouffer, R.J., and John, J.G. (2013). Reductions in labour capacity from heat stress under climate warming. *Nat. Clim. Chang.* *3*, 563–566. <https://doi.org/10.1038/nclimate1827>.
 9. Kjellstrom, T., Maitre, N., Saget, C., Otto, M., and Karimova, T. (2019). Working on a warmer planet: The effect of heat stress on productivity and decent work (International Labor Office). <https://www.ilo.org/publications/major-publications/working-warmer-planet-effect-heat-stress-productivity-and-decent-work>.
 10. Powis, C.M., Byrne, D., Zobel, Z., Gassert, K.N., Lute, A.C., and Schwalm, C.R. (2023). Observational and model evidence together support widespread exposure to noncompensable heat under continued global warming. *Sci. Adv.* *9*, eadg9297. <https://doi.org/10.1126/sciadv.adg9297>.
 11. Raymond, C., Matthews, T., and Horton, R.M. (2020). The emergence of heat and humidity too severe for human tolerance. *Sci. Adv.* *6*, eaaw1838. <https://doi.org/10.1126/sciadv.aaw1838>.
 12. Russo, S., Sillmann, J., and Sterl, A. (2017). Humid heat waves at different warming levels. *Sci. Rep.* *7*, 7477. <https://doi.org/10.1038/s41598-017-07536-7>.
 13. Parsons, L.A., Shindell, D., Tigchelaar, M., Zhang, Y., and Spector, J.T. (2021). Increased labor losses and decreased adaptation potential in a warmer world. *Nat. Commun.* *12*, 7286. <https://doi.org/10.1038/s41467-021-27328-y>.
 14. Takakura, J., Fujimori, S., Takahashi, K., Hasegawa, T., Honda, Y., Hanasaki, N., Hijikata, Y., and Masui, T. (2018). Limited Role of Working Time Shift in Offsetting the Increasing Occupational-Health Cost of Heat Exposure. *Earth's Future* *6*, 1588–1602. <https://doi.org/10.1029/2018EF000883>.
 15. Orlov, A., Sillmann, J., Aunan, K., Kjellstrom, T., and Aaheim, A. (2020). Economic costs of heat-induced reductions in worker productivity due to global warming. *Glob. Environ. Change* *63*, 102087. <https://doi.org/10.1016/j.gloenvcha.2020.102087>.
 16. de Lima, C.Z., Buzan, J.R., Moore, F.C., Baldos, U.L.C., Huber, M., and Hertel, T.W. (2021). Heat stress on agricultural workers exacerbates crop impacts of climate change. *Environ. Res. Lett.* *16*, 044020. <https://doi.org/10.1088/1748-9326/abeb9f>.
 17. Orlov, A., Daloz, A.S., Sillmann, J., Thiery, W., Douzal, C., Lejeune, Q., and Schleussner, C. (2021). Global Economic Responses to Heat Stress Impacts on Worker Productivity in Crop Production. *Econ. Disaster. Clim. Chang.* *5*, 367–390. <https://doi.org/10.1007/s41885-021-00091-6>.
 18. Simpson, C., Hosking, J.S., Mitchell, D., Betts, R.A., and Shuckburgh, E. (2021). Regional disparities and seasonal differences in climate risk to rice labour. *Environ. Res. Lett.* *16*, 124004. <https://doi.org/10.1088/1748-9326/ac3288>.
 19. Hasegawa, T., Fujimori, S., Havlík, P., Valin, H., Bodirsky, B.L., Doelman, J.C., Fellmann, T., Kyle, P., Koopman, J.F.L., Lotze-Campen, H., et al. (2018). Risk of increased food insecurity under stringent global climate change mitigation policy. *Nat. Clim. Chang.* *8*, 699–703. <https://doi.org/10.1038/s41558-018-0230-x>.
 20. Nelson, G.C., Valin, H., Sands, R.D., Havlík, P., Ahammad, H., Deryng, D., Elliott, J., Fujimori, S., Hasegawa, T., Heyhoe, E., et al. (2014). Climate change effects on agriculture: Economic responses to biophysical shocks. *Proc. Natl. Acad. Sci. USA* *111*, 3274–3279. <https://doi.org/10.1073/pnas.1222465110>.
 21. Wiebe, K., Lotze-Campen, H., Sands, R., Tabeau, A., van der Mensbrugge, D., Biewald, A., Bodirsky, B., Islam, S., Kavallari, A., Mason-D'Croz, D., et al. (2015). Climate change impacts on agriculture in 2050 under a range of plausible socioeconomic and emissions scenarios. *Environ. Res. Lett.* *10*, 085010. <https://doi.org/10.1088/1748-9326/10/8/085010>.
 22. Eyring, V., Bony, S., Meehl, G.A., Senior, C.A., Stevens, B., Stouffer, R.J., and Taylor, K.E. (2016). Overview of the Coupled Model Intercomparison Project Phase 6 (CMIP6) experimental design and organization. *Geosci. Model Dev. (GMD)* *9*, 1937–1958. <https://doi.org/10.5194/gmd-9-1937-2016>.
 23. Aaheim, H.A., Orlov, A., Wei, T., and Glomsrød, S. (2018). GRACE model and applications. *CICERO Report;2018:01* (CICERO Center for International Climate Research), pp. 1–45.
 24. Aguiar, A., Narayanan, B., and McDougall, R. (2016). An Overview of the GTAP 9 Data Base. *J. Glob. Econ. Anal.* *1*, 181–208. <https://doi.org/10.21642/JGEA.010103AF>.
 25. Andreyeva, T., Long, M.W., and Brownell, K.D. (2010). The Impact of Food Prices on Consumption: A Systematic Review of Research on the Price Elasticity of Demand for Food. *Am. J. Public Health* *100*, 216–222. <https://doi.org/10.2105/AJPH.2008.151415>.
 26. Liu, M., Shamdasani, Y., and Taraz, V. (2023). Climate Change and Labor Reallocation: Evidence from Six Decades of the Indian Census. *Am. Econ. J. Econ. Policy* *15*, 395–423. <https://doi.org/10.1257/pol.20210129>.
 27. Müller, C., and Robertson, R.D. (2014). Projecting future crop productivity for global economic modeling. *Agric. Econ.* *45*, 37–50. <https://doi.org/10.1111/agec.12088>.
 28. Moore, F.C., Baldos, U., Hertel, T., and Diaz, D. (2017). New science of climate change impacts on agriculture implies higher social cost of carbon. *Nat. Commun.* *8*, 1607. <https://doi.org/10.1038/s41467-017-01792-x>.
 29. Moore, F.C., Baldos, U.L.C., and Hertel, T. (2017). Economic impacts of climate change on agriculture: a comparison of process-based and statistical yield models. *Environ. Res. Lett.* *12*, 065008. <https://doi.org/10.1088/1748-9326/aa6eb2>.
 30. Li, L., Wang, B., Feng, P., Jägermeyr, J., Asseng, S., Müller, C., Macadam, I., Liu, D.L., Waters, C., Zhang, Y., et al. (2023). The optimization of model ensemble composition and size can enhance the robustness of crop yield projections. *Commun. Earth Environ.* *4*, 362. <https://doi.org/10.1038/s43247-023-01016-9>.
 31. Fujimori, S., Iizumi, T., Hasegawa, T., Takakura, J., Takahashi, K., and Hijikata, Y. (2018). Macroeconomic Impacts of Climate Change Driven by Changes in Crop Yields. *Sustainability* *10*, 3673. <https://doi.org/10.3390/su10103673>.
 32. Zabel, F., Müller, C., Elliott, J., Minoli, S., Jägermeyr, J., Schneider, J.M., Franke, J.A., Moyer, E., Dury, M., Francois, L., et al. (2021). Large potential for crop production adaptation depends on available future varieties. *Glob. Chang. Biol.* *27*, 3870–3882. <https://doi.org/10.1111/gcb.15649>.

33. Hallegatte, S., and Rozenberg, J. (2017). Climate change through a poverty lens. *Nat. Clim. Chang.* 7, 250–256. <https://doi.org/10.1038/nclimate3253>.
34. Hertel, T.W., Burke, M.B., and Lobell, D.B. (2010). The poverty implications of climate-induced crop yield changes by 2030. *Glob. Environ. Change* 20, 577–585. <https://doi.org/10.1016/j.gloenvcha.2010.07.001>.
35. Falkendal, T., Otto, C., Schewe, J., Jägermeyr, J., Konar, M., Kummu, M., Watkins, B., and Puma, M.J. (2021). Grain export restrictions during COVID-19 risk food insecurity in many low- and middle-income countries. *Nat. Food* 2, 11–14. <https://doi.org/10.1038/s43016-020-00211-7>.
36. Janssens, C., Havlík, P., Krisztin, T., Baker, J., Frank, S., Hasegawa, T., Leclère, D., Ohrel, S., Ragnauth, S., Schmid, E., et al. (2020). Global hunger and climate change adaptation through international trade. *Nat. Clim. Chang.* 10, 829–835. <https://doi.org/10.1038/s41558-020-0847-4>.
37. Stevanović, M., Popp, A., Lotze-Campen, H., Dietrich, J.P., Müller, C., Bonsch, M., Schmitz, C., Bodirsky, B.L., Humpenöder, F., and Weindl, I. (2016). The impact of high-end climate change on agricultural welfare. *Sci. Adv.* 2, e1501452. <https://doi.org/10.1126/sciadv.1501452>.
38. Lafferty, D.C., Sriver, R.L., Haqiqi, I., Hertel, T.W., Keller, K., and Nicholas, R.E. (2021). Statistically bias-corrected and downscaled climate models underestimate the adverse effects of extreme heat on U.S. maize yields. *Commun. Earth Environ.* 2, 196. <https://doi.org/10.1038/s43247-021-00266-9>.
39. Schewe, J., Gosling, S.N., Reyer, C., Zhao, F., Ciais, P., Elliott, J., Francois, L., Huber, V., Lotze, H.K., Seneviratne, S.I., et al. (2019). State-of-the-art global models underestimate impacts from climate extremes. *Nat. Commun.* 10, 1005. <https://doi.org/10.1038/s41467-019-08745-6>.
40. Shindell, D., Ru, M., Zhang, Y., Seltzer, K., Faluvegi, G., Nazarenko, L., Schmidt, G.A., Parsons, L., Challapalli, A., Yang, L., and Glick, A. (2021). Temporal and spatial distribution of health, labor, and crop benefits of climate change mitigation in the United States. *Proc. Natl. Acad. Sci. USA* 118, e2104061118. <https://doi.org/10.1073/pnas.2104061118>.
41. Gilbert, J., and Oladi, R. (2009). Capital specificity, imperfect labor mobility and growth in developing economies. *Int. Rev. Econ. Finance* 18, 113–122. <https://doi.org/10.1016/j.iref.2007.06.008>.
42. Hertel, T.W., and de Lima, C.Z. (2020). Viewpoint: Climate impacts on agriculture: Searching for keys under the streetlight. *Food Pol.* 95, 101954. <https://doi.org/10.1016/j.foodpol.2020.101954>.
43. Zabel, F., and Poschod, B. (2023). The Teddy tool v1.1: temporal disaggregation of daily climate model data for climate impact analysis. *Geosci. Model Dev. (GMD)* 16, 5383–5399. <https://doi.org/10.5194/gmd-16-5383-2023>.
44. Armington, P.S. (1969). A Theory of Demand for Products Distinguished by Place of Production (Une theorie de la demande de produits differencies d'apres leur origine) (Una teoria de la demanda de productos distinguiendolos segun el lugar de produccion). *Staff Pap. Int. Monet. Fund* 16, 159–178. <https://doi.org/10.2307/3866403>.
45. Zhang, T., van der Wiel, K., Wei, T., Screen, J., Yue, X., Zheng, B., Selten, F., Bintanja, R., Anderson, W., Blackport, R., et al. (2022). Increased wheat price spikes and larger economic inequality with 2°C global warming. *One Earth* 5, 907–916. <https://doi.org/10.1016/j.oneear.2022.07.004>.
46. Wei, T., and Liu, Y. (2017). Estimation of global rebound effect caused by energy efficiency improvement. *Energy Econ.* 66, 27–34. <https://doi.org/10.1016/j.eneco.2017.05.030>.
47. O'Neill, B.C., Tebaldi, C., van Vuuren, D.P., Eyring, V., Friedlingstein, P., Hurtt, G., Knutti, R., Kriegler, E., Lamarque, J.-F., Lowe, J., et al. (2016). The Scenario Model Intercomparison Project (ScenarioMIP) for CMIP6. *Geosci. Model Dev. (GMD)* 9, 3461–3482. <https://doi.org/10.5194/gmd-9-3461-2016>.
48. Jägermeyr, J., Müller, C., Minoli, S., Ray, D., and Siebert, S. (2021). GGCM Phase 3 crop calendar. Zenodo. <https://doi.org/10.5281/zenodo.5062513>.
49. Hausfather, Z., and Peters, G.P. (2020). Emissions – the ‘business as usual’ story is misleading. *Nature* 577, 618–620. <https://doi.org/10.1038/d41586-020-00177-3>.
50. Meehl, G.A., Senior, C.A., Eyring, V., Flato, G., Lamarque, J.-F., Stouffer, R.J., Taylor, K.E., and Schlund, M. (2020). Context for interpreting equilibrium climate sensitivity and transient climate response from the CMIP6 Earth system models. *Sci. Adv.* 6, eaba1981. <https://doi.org/10.1126/sciadv.aba1981>.
51. IFPRI (2020). Global Spatially-Disaggregated Crop Production Statistics Data for 2010 Version 2.0 (Harvard Dataverse). <https://doi.org/10.7910/DVN/PRFF8V>.
52. Stull, R. (2011). Wet-Bulb Temperature from Relative Humidity and Air Temperature. *J. Appl. Meteorol. Climatol.* 50, 2267–2269. <https://doi.org/10.1175/JAMC-D-11-0143.1>.
53. Moran, D.S., Pandolf, K.B., Shapiro, Y., Heled, Y., Shani, Y., Mathew, W.T., and Gonzalez, R.R. (2001). An environmental stress index (ESI) as a substitute for the wet bulb globe temperature (WBGT). *J. Therm. Biol.* 26, 427–431. [https://doi.org/10.1016/S0306-4565\(01\)00055-9](https://doi.org/10.1016/S0306-4565(01)00055-9).
54. Kong, Q., and Huber, M. (2022). Explicit Calculations of Wet-Bulb Globe Temperature Compared With Approximations and Why It Matters for Labor Productivity. *Earth's Future* 10, e2021EF002334. <https://doi.org/10.1029/2021EF002334>.
55. Moran, D.S., and Epstein, Y. (2006). Evaluation of the environmental stress index (ESI) for hot/dry and hot/wet climates. *Ind. Health* 44, 399–403. <https://doi.org/10.2486/indhealth.44.399>.
56. Kjellstrom, T., Gabrys, S., Lemke, B., and Dear, K. (2009). The ‘Hothaps’ programme for assessing climate change impacts on occupational health and productivity: an invitation to carry out field studies. *Glob. Health Action* 2, 2082. <https://doi.org/10.3402/gha.v2i0.2082>.
57. Bröde, P., Fiala, D., Lemke, B., and Kjellstrom, T. (2018). Estimated work ability in warm outdoor environments depends on the chosen heat stress assessment metric. *Int. J. Biometeorol.* 62, 331–345. <https://doi.org/10.1007/s00484-017-1346-9>.
58. Kjellstrom, T., Holmer, I., and Lemke, B. (2009). Workplace heat stress, health and productivity – an increasing challenge for low and middle-income countries during climate change. *Glob. Health Action* 2. <https://doi.org/10.3402/gha.v2i0.2047>.
59. NIOSH (1986). *Criteria for a recommended standard: occupational exposure to hot environments*. NIOSH Publication No. 86-113 (National Institute of Occupational Health).
60. Foster, J., Smallcombe, J.W., Hodder, S., Jay, O., Flouris, A.D., Nybo, L., and Havenith, G. (2021). An advanced empirical model for quantifying the impact of heat and climate change on human physical work capacity. *Int. J. Biometeorol.* 65, 1215–1229. <https://doi.org/10.1007/s00484-021-02105-0>.

One Earth, Volume 7

Supplemental information

**Human heat stress could offset potential
economic benefits of CO₂ fertilization in crop
production under a high-emissions scenario**

Anton Orlov, Jonas Jägermeyr, Christoph Müller, Anne Sophie Daloz, Florian Zabel, Sara Minoli, Wenfeng Liu, Tzu-Shun Lin, Atul K. Jain, Christian Folberth, Masashi Okada, Benjamin Pöschl, Andrew Smerald, Julia M. Schneider, and Jana Sillmann

Supplementary Information

Contents

Supplementary Experimental Procedures	2
Supplementary Tables	8
Supplementary Figures.....	9

Supplemental Experimental Procedures

Daily mean vs. hourly responses

Bias-adjusted hourly climate model data is not available. Therefore, we use daily mean values. To test our results for a potential underestimation, we apply the Teddy-tool v1.1 (TEmporal Disaggregation of Daily Climate Model Data) for temporal disaggregation of daily ISIMIP3b climate model data to hourly timeseries ¹. The applied method for disaggregation compares every single day of a given climate model dataset to daily bias-adjusted WFDE5 reanalysis data (1980-2019). For the day of interest at a specific location, the Teddy-Tool identifies the most similar climatic day at the same location within a predefined time window (+/- 5 days) around the day of interest. For the best fit, it applies the historical hourly diurnal profile (based on bias-adjusted hourly WFDE5 reanalysis data) to the climate model daily mean value. Thereby, the Teddy-Tool conserves mass and energy in all cases and strictly preserves the daily mean value (sum for precipitation) of the climate model. The physical relationship between temperature and relative humidity is considered and oversaturation is restricted. For radiation, precalculated potential incoming shortwave radiation is set as a maximum. For temperature, daily maximum, minimum, and mean values of the climate model are considered for the temporal disaggregation and are exactly reproduced in the sub-daily results. Thus, the Teddy-Tool allows for incorporating local sub-daily climate profiles and therefore reproducing seasonal and regional characteristics.

Then, we compare the levels of labour capacity based on daily and disaggregated hourly data. For this sensitivity analysis, we exemplarily selected RCP 7.0 of the UKESM1-0-LL climate model for 30 locations representing major global agricultural regions (see Fig. S11). Assuming a 7 a.m. to 7 p.m. workday, we find that, indeed, when using hourly data, the heat-induced labour losses could be substantially larger than when using the daily mean depending on latitude and season (see Fig. S12). The largest difference can be found in the summer seasons of continental climate zones (up to 30 percentage points), while tropical regions show lower and more uniform reductions throughout the year. However, we do not allow for shifts in the working hours, which could partly compensate heat-induced labour losses.

Description of the production system in GRACE

Here, we description the production system for crops, which is implemented in GRACE. For irrigated crops, we adopt the structure of crop production similar to Luckmann et al. (2014) and

Orlov et al. (2021), which is illustrated in Fig. 1. Rainfed crops have the same production structure but without water as a production input. Sectoral production is modelled using nested constant elasticity of substitution (CES) functions. Adaptation in production is represented by substitution among production inputs (i.e., labour, capital, and land) as well as mobility of production inputs across sectors. Elasticities of substitution implemented in CES functions determine the degree of substitutability among production inputs. The substitution effect is determined by the value of substitution elasticity and the value share of production input.

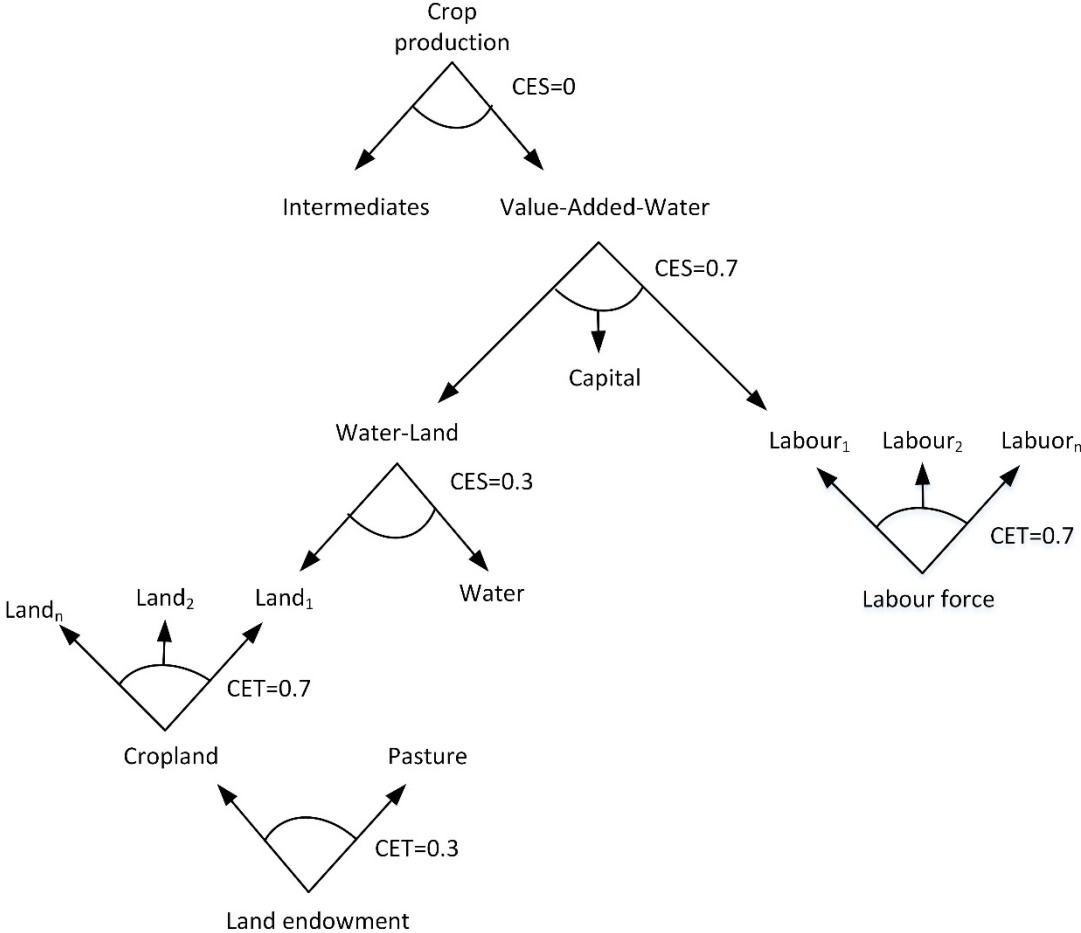


Fig. 1: Nested structure of production of irrigated crops.

At the top level of nested CES functions, production of crops is described by a Leontief production function over intermediates and the aggregate of value-added-water, which implies no substitutability between those two aggregates. At the second level, the aggregate of value-added-water (VAW_i) is a standard CES function over capital (see Eq. 1). In GRACE, equations are also region- and sector specific, and the indexes defining region and sector are removed from Eq. 1 for simplicity.

$$VAW = ad * [sh_f * WL^r + sh_f * C^r + sh_f * L^r]^{\frac{1}{r}} \tag{Eq. 1}$$

where

VAW is the value-added aggregate in a sector

WL is the aggregate of water-land in a sector

C is capital input in a sector

L is labour input in a sector

ad is the shifter parameter for CES function in a sector

sh is the factor-specific share parameter in a sector

r is the elasticity parameter, which equals to: $r = 1 - \frac{1}{\sigma}$

σ is the substitution elasticity

The elasticity of substitution between capital, labour, and the aggregate of water-land, which measures the change in the ratio of inputs with respect to the ratio of their prices, is assumed to equal 0.7. The empirical literature rejects the hypothesis of a Cobb-Douglas function, which implies a substitution elasticity between capital and labour of one, and shows that the substitution elasticity tends to be less than one^{4,5}. In GRACE, the default value of the substitution elasticity between capital, labour, and the aggregate of water-land is assumed to equal 0.7, which is supported by empirical evidence⁶⁻⁸. At the third level, the aggregate of water-land is depicted by a standard CES function over water and land. The substitution elasticity between water and land tends to have a small value ranking from 0 to 0.3^{2,9,10}. In our analysis, the value of this substitution elasticity is assumed to equal 0.3.

The allocation of land among sectors is modelled using a two-level nested constant elasticity of transformation (CET) function. At the first level, land is allocated between cropland and other sectors (e.g., pasture) using a CET function with a transformation elasticity of 0.3. At the second level, a CET function allocates cropland among different types of crops. In different CGE-based studies, the value of transformation elasticity for cropland among different types of crops varies from 0 to 1¹⁰⁻¹⁵. In our analysis, the value of transformation elasticity for cropland is assumed to equal 0.7. Following Gaasland (2008), labour allocation is modelled to be imperfectly mobile across sectors using a constant elasticity of transformation (CET) function with a transformation elasticity of 3.

Description of the price system in GRACE

Equilibrium prices are determined by interactions of demand and supply. In CGE models, equilibrium in commodity and factor markets are achieved when three main conditions are satisfied, such as i) market clearance (i.e., demand should be equal supply), ii) zero profit (i.e., production revenues should be equal production costs), and iii) income balance (i.e.,

consumer's income should be equal expenditures). These conditions are achieved through market mechanisms and adjustments, such as mobility (re-allocation) production factors (i.e., labour, capital, and land) across sectors, substitution among production factors, changes in trade and consumption, and substitution in consumption of commodities.

Producer prices are determined by unit cost of production inputs, such as intermediates, labour, capital, and land. For example, the price formation of irrigated crops is shown in Fig. 2. The producer price of an irrigated crop (PD) is determined by an aggregate price of intermediates (PIO) and an aggregate price of value-added including water (PVAW). The price of value-added is determined by factor prices for capital, labour, and land (PFA_f) and the price of water input (P_{water}). The consumer price of a crop (P) is determined by a domestic producer price (PD) and an import price of crop (PIM). GRACE is formulated as a mixed-complementarity problem (MCP) ¹⁷⁻¹⁹. Commodity and factor prices are defined as the complementary variables to zero profit conditions for commodity and factor markets, while the aggregate prices, such as the price of value-added, is defined as unit cost functions derived from CES functions (Eq. 2). Note that in GRACE, equations are region- and sector specific, and the indexes defining region and sector are removed from Eq. 2 for simplicity.

$$PVAW = \frac{1}{ad} * [sh^\sigma * PWL^{1-\sigma} + sh_{capital}^\sigma * PFA_{capital}^{1-\sigma} + sh_{labour}^\sigma * PFA_{labour}^{1-\sigma}]^{\frac{1}{1-\sigma}}$$

Eq. 2

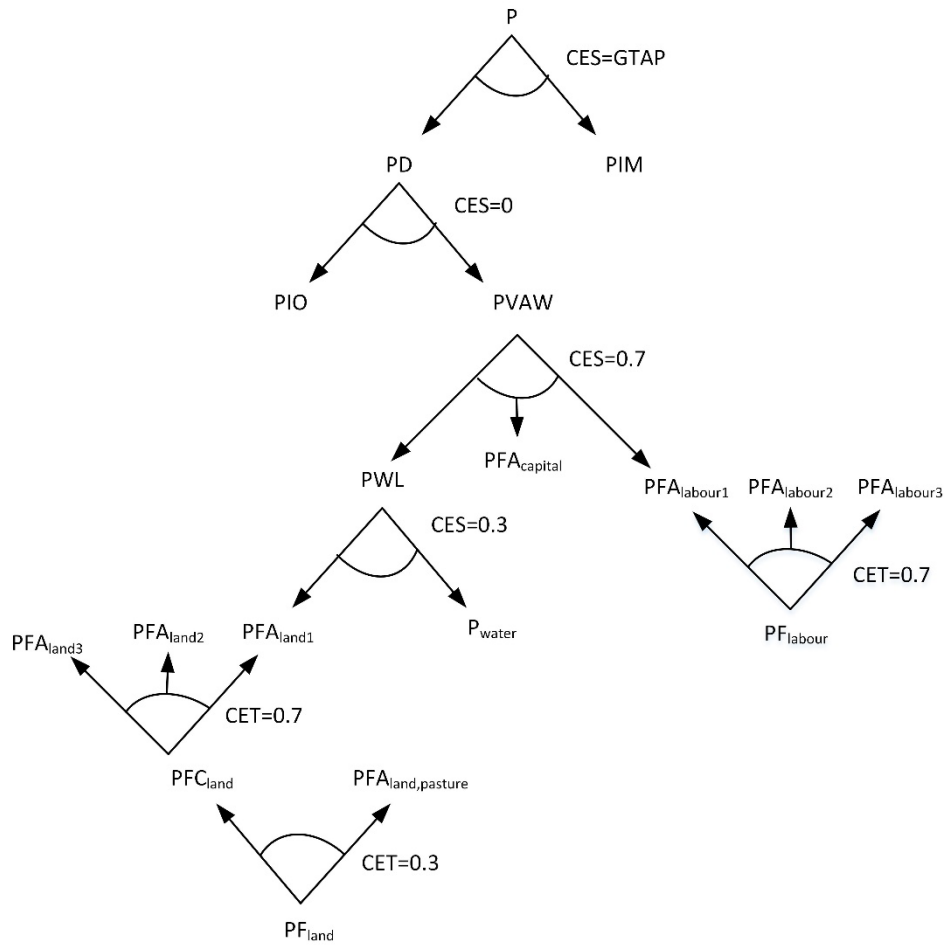


Fig. 2: Price system for irrigated crops.

A productivity shock affects the production cost (PD) and the returns to factors of production (i.e., wages and profit) (PFA_f). To minimise the cost, producers adjust their production through substitution of inputs as well as factor mobility. In response to changes in producer prices and income, consumers adjust their consumption by choosing how much and what to consume. Imported and domestically produced commodities are assumed to be imperfect substitutes, which is modelled using the Armington approach (i.e., CES functions). The elasticity of substitution between imported and domestic commodities are obtained from the GTAP database. Moreover, different commodities (e.g., different crops or food vs. non-food) are assumed to be imperfect substitutes in private consumption (i.e., substitution effect). Moreover, a demand response of staple crops is also determined by changes in relative prices of staple crops and other goods (i.e., food and non-food). For example, in rich countries, people would consume more “luxury” items if food becomes cheaper (i.e., income effect). Changes in commodity and factor prices lead to a new market equilibrium through re-allocation of production inputs across sectors, substitution effects, and changes in trade and consumption

patterns. Substitution effects in production and consumption of commodities induce non-linearity in economic responses.

Formation of consumer prices

In the GRACE model, the price response is determined by interactions between demand and supply, given the assumption of market equilibrium (i.e., demand equals supply) (Fig. 3). As the GRACE model explicitly depicts bilateral trade, the demand for commodities consists of domestic supply (minus export) and import. In the presence of trade, in addition to domestic production, the response of global supply of crops also determines the response of consumer prices. Similar to other CGE models, in GRACE, domestic and imported commodities are assumed to be imperfect substitutes and therefore, the price response differs by region, depending on the share of imported commodities in total consumption and the shock on crop productivity. The response of consumer prices and domestic production can be asymmetric because of trade possibility. For example, a region can experience a climate-induced reduction in production of crops and, at the same time, a reduction in the consumer price, if there is a global increase in production, leading to a higher import demand. However, if the yield shock is relatively strong and the domestic demand is mainly satisfied through the domestic supply, then a reduction in domestic production could lead to an increase in the regional consumer price of crops due to imperfect substitutability between domestically produced and imported crops.

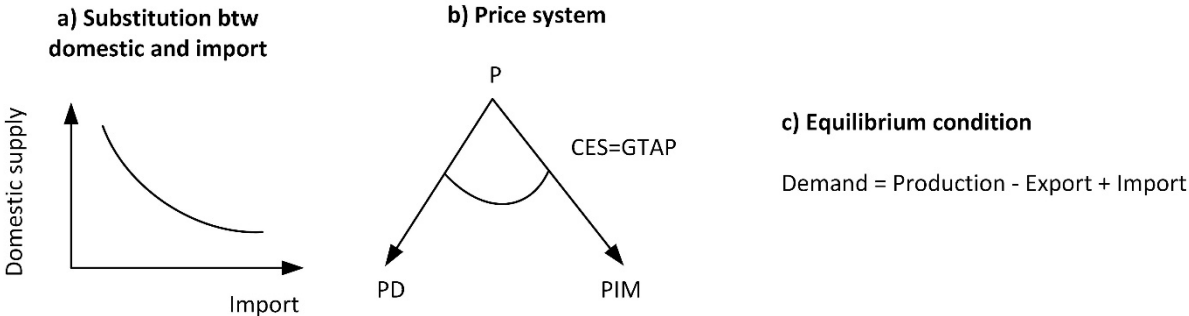


Fig. 3: Formation of consumer prices.

Supplementary Tables

Table S1: Regional aggregation.

Regions	Countries
W-Europe (Western Europe)	Albania, Austria, Belgium, Switzerland, Germany, Denmark, Spain, Estonia, Finland, France, United Kingdom, Greece, Croatia, Ireland, Italy, Lithuania, Luxembourg, Latvia, Netherlands, Norway, Portugal, Slovenia, Sweden
W-Asia (Western Asia)	United Arab Emirates, Armenia, Azerbaijan, Cyprus, Georgia, Israel, Jordan, Kuwait, Oman, Qatar, Saudi Arabia, Turkey, Iraq, Lebanon, Syria, Yemen
L-America (Latin America)	Argentina, Bolivia, Brazil, Chile, Colombia, Costa Rica, Dominican Republic, Ecuador, Guatemala, Honduras, Jamaica, Mexico, Nicaragua, Panama, Peru, Puerto Rico, Paraguay, El Salvador, Trinidad & Tobago, Uruguay, Venezuela
Oceania	Australia, New Zealand
Africa	Benin, Burkina Faso, Botswana, Côte d'Ivoire, Cameroon, Egypt, Ethiopia, Ghana, Kenya, Morocco, Madagascar, Mozambique, Mauritius, Malawi, Namibia, Nigeria, Rwanda, Senegal, Togo, Tunisia, Tanzania, Uganda, Angola, Congo - Kinshasa, Chad, Congo - Brazzaville, Equatorial Guinea, Gabon, São Tomé & Príncipe, Central African Republic, Burundi, Comoros, Djibouti, Eritrea, Mayotte, Seychelles, Somalia, Sudan, South Sudan, Algeria, Libya, Cape Verde, Gambia, Guinea-Bissau, Mali, Mauritania, Niger, St. Helena, Sierra Leone, South Africa, Zambia, Zimbabwe
S-Asia (Southern Asia)	Bangladesh, India, Iran, Sri Lanka, Nepal, Pakistan, Afghanistan, Bhutan, Maldives
E-Europe (Russia and Eastern Europe)	Bulgaria, Belarus, Czechia, Hungary, Poland, Romania, Russia, Slovakia, Ukraine
SE-Asia (South-East Asia)	Brunei, Indonesia, Cambodia, Laos, Malaysia, Philippines, Thailand, Vietnam, Myanmar (Burma)
N-America (North America)	Canada, United States
E-Asia (East Asia)	China, Hong Kong SAR China, Japan, South Korea, Mongolia, Taiwan
C-Asia (Central Asia)	Kazakhstan, Kyrgyzstan, Tajikistan, Turkmenistan, Uzbekistan

Supplementary Figures

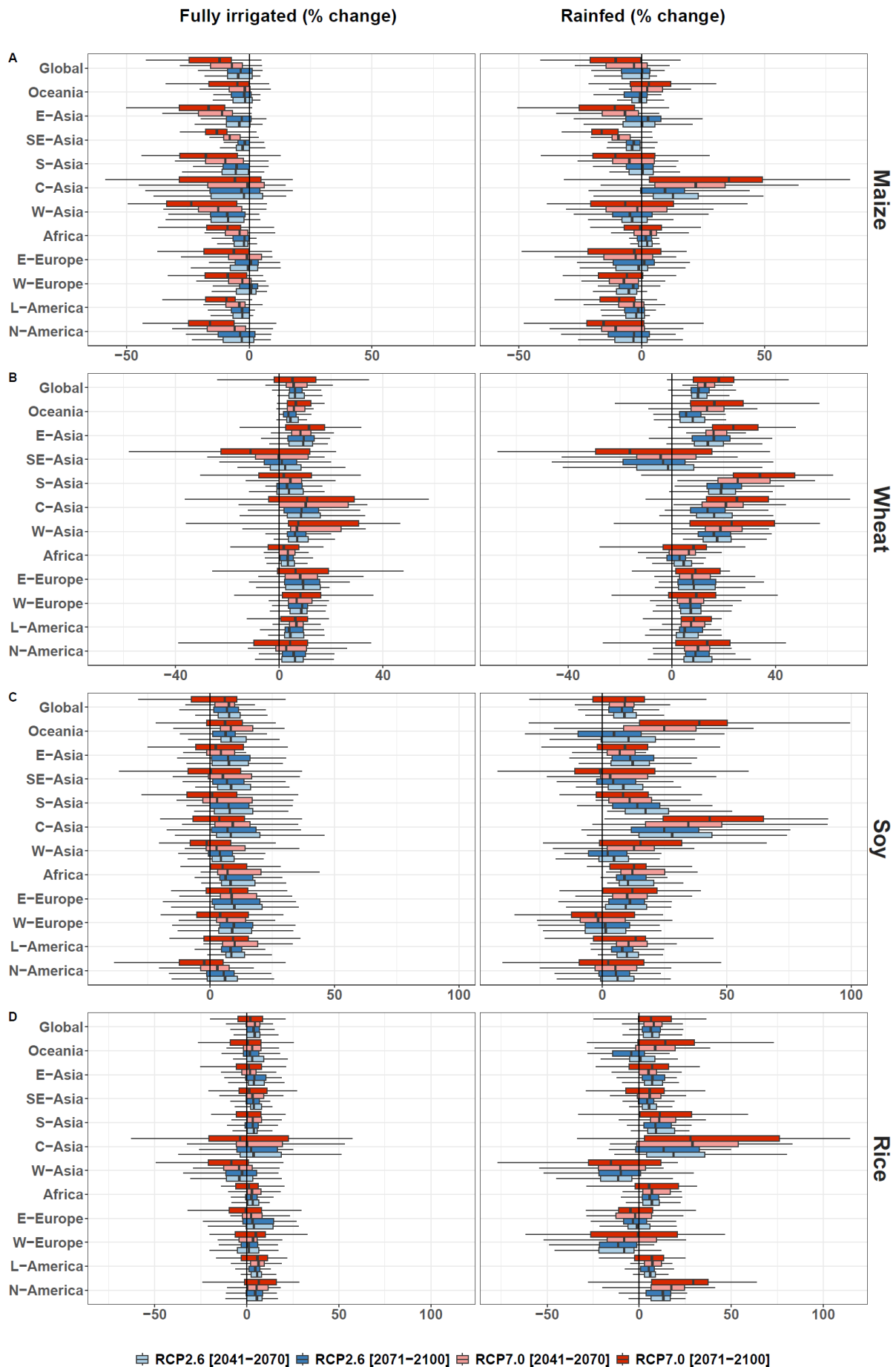


Fig. S1: Multi-year mean changes in regional harvested-area-weighted yields of fully irrigated and rainfed maize (A), wheat (B), soy (C), and rice (D) by the mid [2041–2070] and end [2071–2100] of the century under RCP2.6 (blue) and RCP7.0 (red) relative to the average yield in the historical time period [1981-2010]. The boxes show the interquartile range across climate and crop model ensembles.

The whiskers show the variability outside the 1st and 3rd quantiles, and outliers are removed.

Share of imported crop in total expenditures on crop consumption

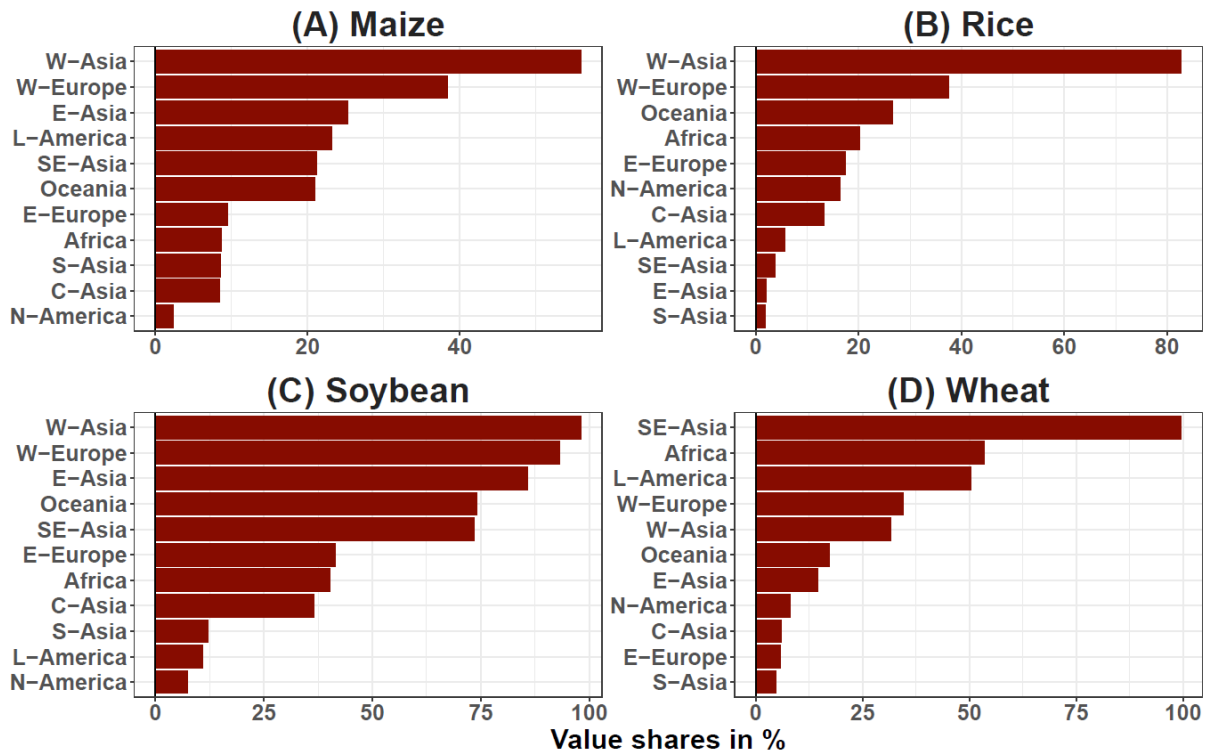


Fig. S2: Shares of imported maize (A), rice (B), soybean (C), and wheat (D) in total expenditures on imported and domestically produced crops (in percent). Own calculations based on version 9 of the GTAP database for 2011 reference period.

Input shares in total production cost

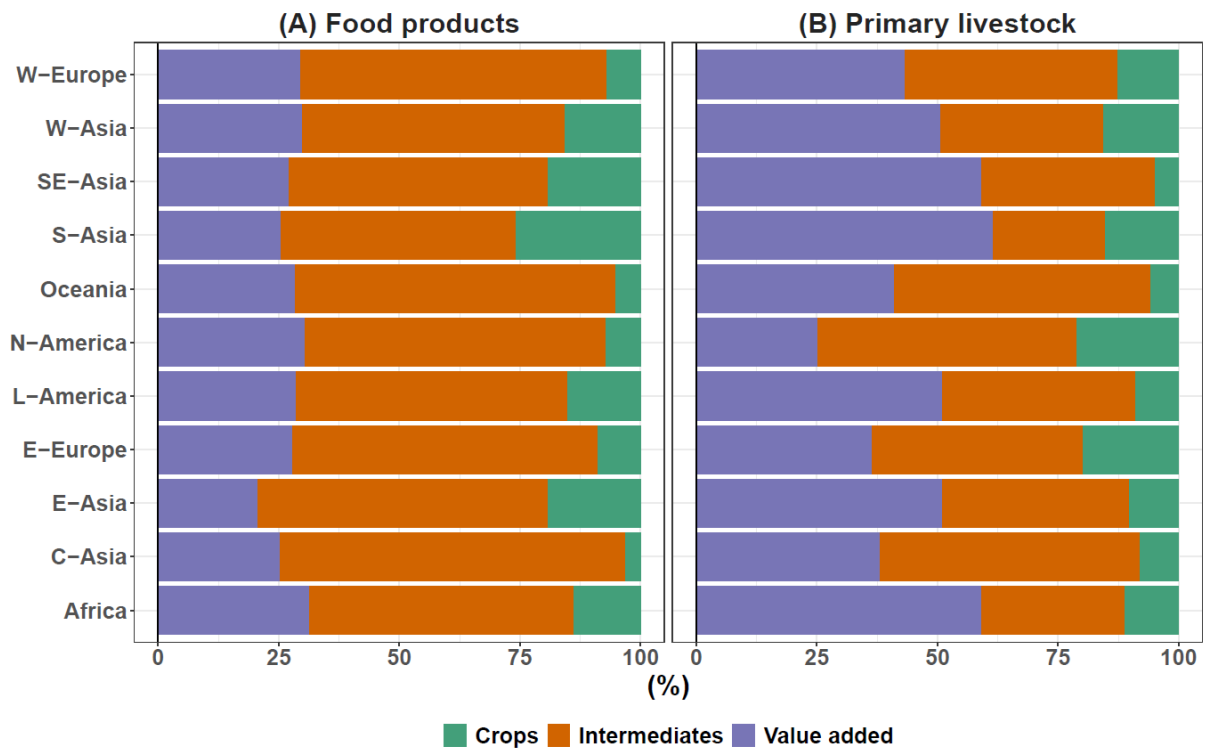


Fig. S3: Shares of crops, intermediates, and value added in total production cost of food products (A) and primary livestock (B) (in percent). Own calculations based on version 9 of the GTAP database for 2011 reference period.

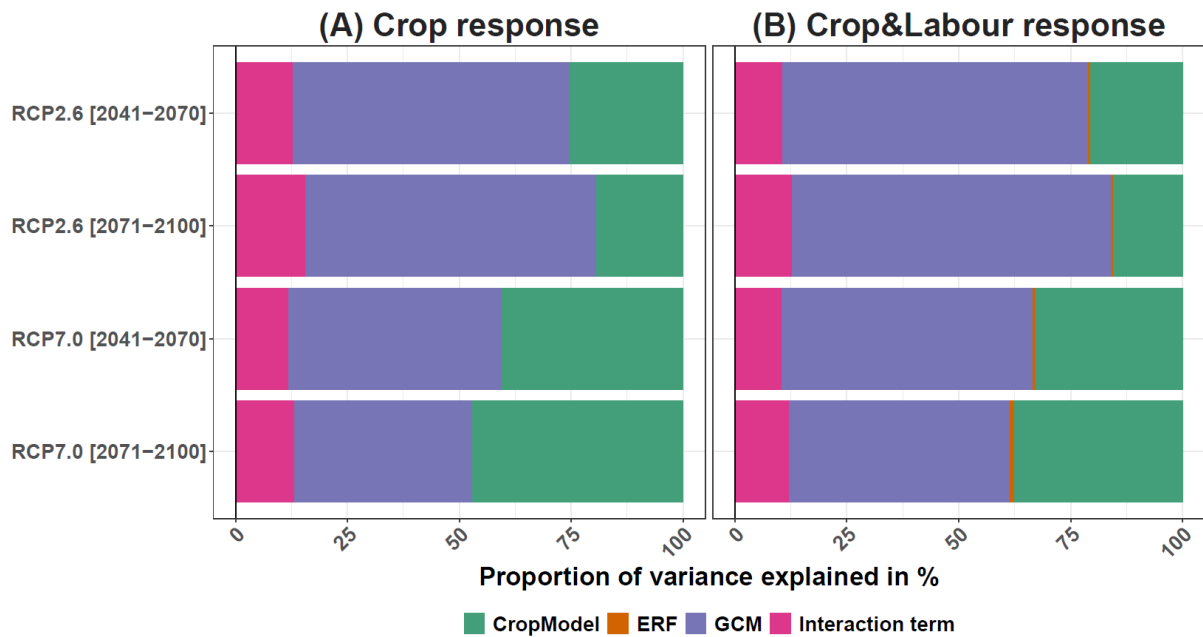


Fig. S4: Analysis of variance for global real income. The legend “GCM” stands for the GCM-related uncertainty, “CropModel” is for the uncertainty of crop model simulations “ERF” is for the uncertainty of heat-labour exposure response functions. “Crop response” (A) show the scenarios that only consider the climate-related yield responses of the four crops. The triangles in shades of orange labelled “Crop&Labour response” (B) show the scenarios that consider both yield changes and heat stress impacts on labour of the four crops.

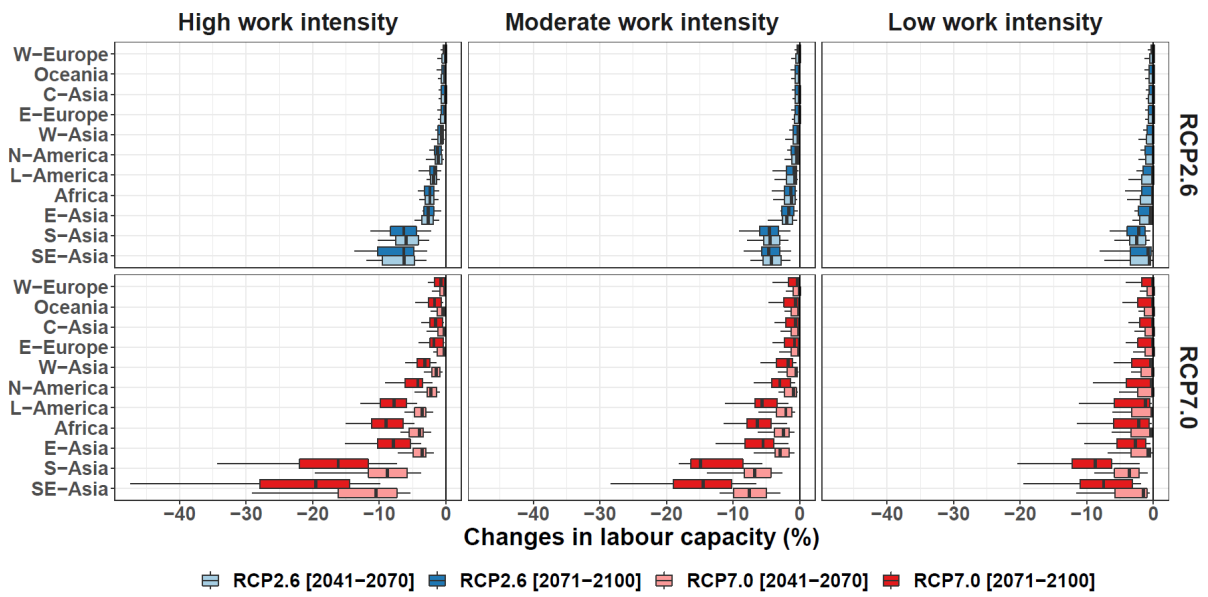


Fig. S5: Area-weighted multi-year mean changes in labour capacity in production of all crops by the mid [2041–2070] and end [2071–2100] of the century under RCP2.6 (blue) and RCP7.0 (red) relative to the average yield in the historical time period [1981–2010]. The boxes show the interquartile range across climate models ensemble and labour-heat exposure-response functions. The whiskers show the variability outside the 1st and 3rd quantiles. The dots show outliers.

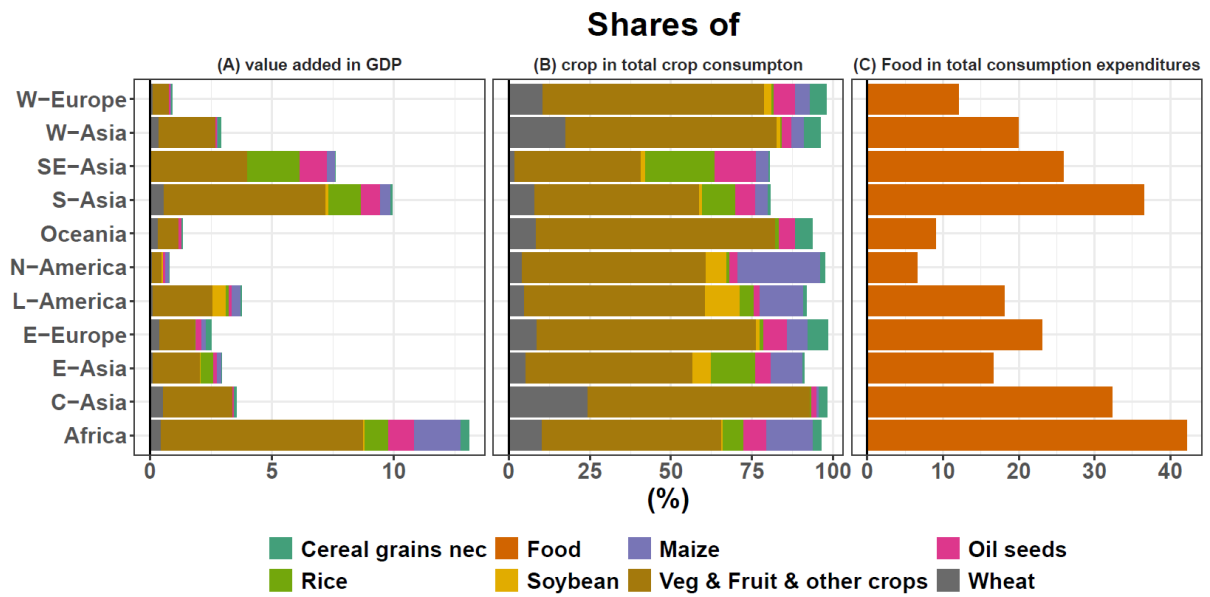


Fig. S6: Shares of value added in GDP (A), shares of crops in total expenditures on crop consumption (B), and shares of food in total consumption expenditures (C) (in percent). Own calculations based on version 9 of the GTAP database for 2011 reference period.

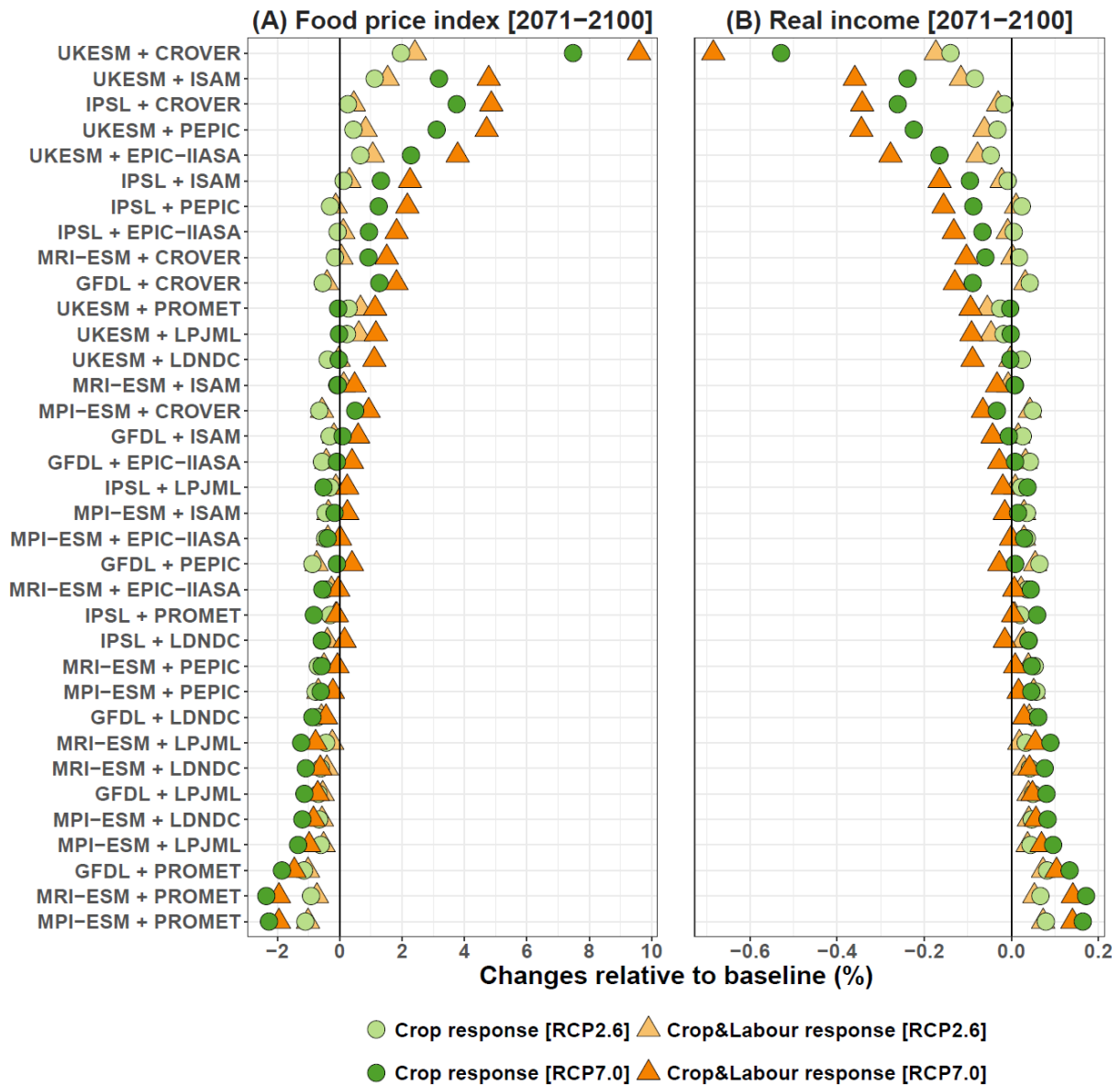


Fig. S7: Median responses of global food price index (A) and real income (B) by the end [2071–2100] of the century under RCP2.6 and RCP7.0 for each climate and crop model combination relative to the historical time period. The income and price responses are simulated using GRACE and show the median changes over GCMs, crop models, and exposure-response functions relative to the state of the world economy in 2011. The circles in shades of green labelled “Crop response” show the scenarios that only consider the climate-related yield responses of the four crops. The triangles in shades of orange labelled “Crop&Labour response” show the scenarios that consider both yield changes and heat stress impacts on labour of the four crops.

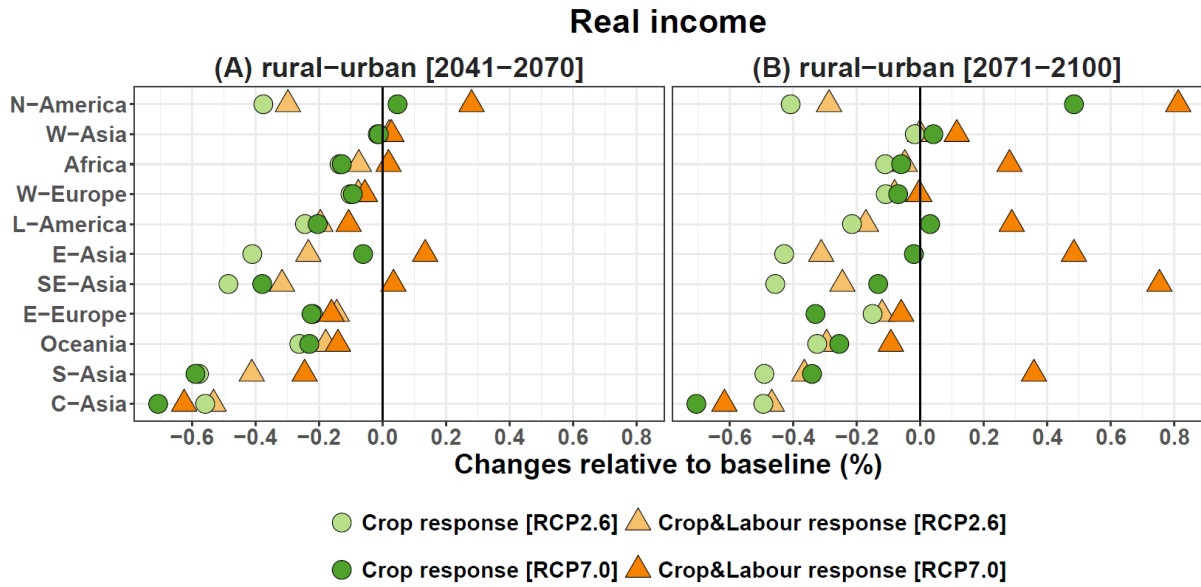


Fig. S8: Median responses of changes in the rural-urban income ratio by the mid [2040–2070] (A) and end [2071–2100] (B) of the century under RCP2.6 and RCP7.0 relative to the historical time period. The income responses are simulated using the GRACE model and show the median changes over GCMs, and crop models, and exposure-response functions relative to the state of the world economy in 2011. The circles in shades of green labelled “Crop response” show the scenarios that only consider the climate-related yield responses of the four crops. The triangles in shades of orange labelled “Crop&Labour response” show the scenarios that consider both yield changes and heat stress impacts on labour of the four crops. A positive (negative) number means that a decrease (increase) in income gap between rural and urban households.

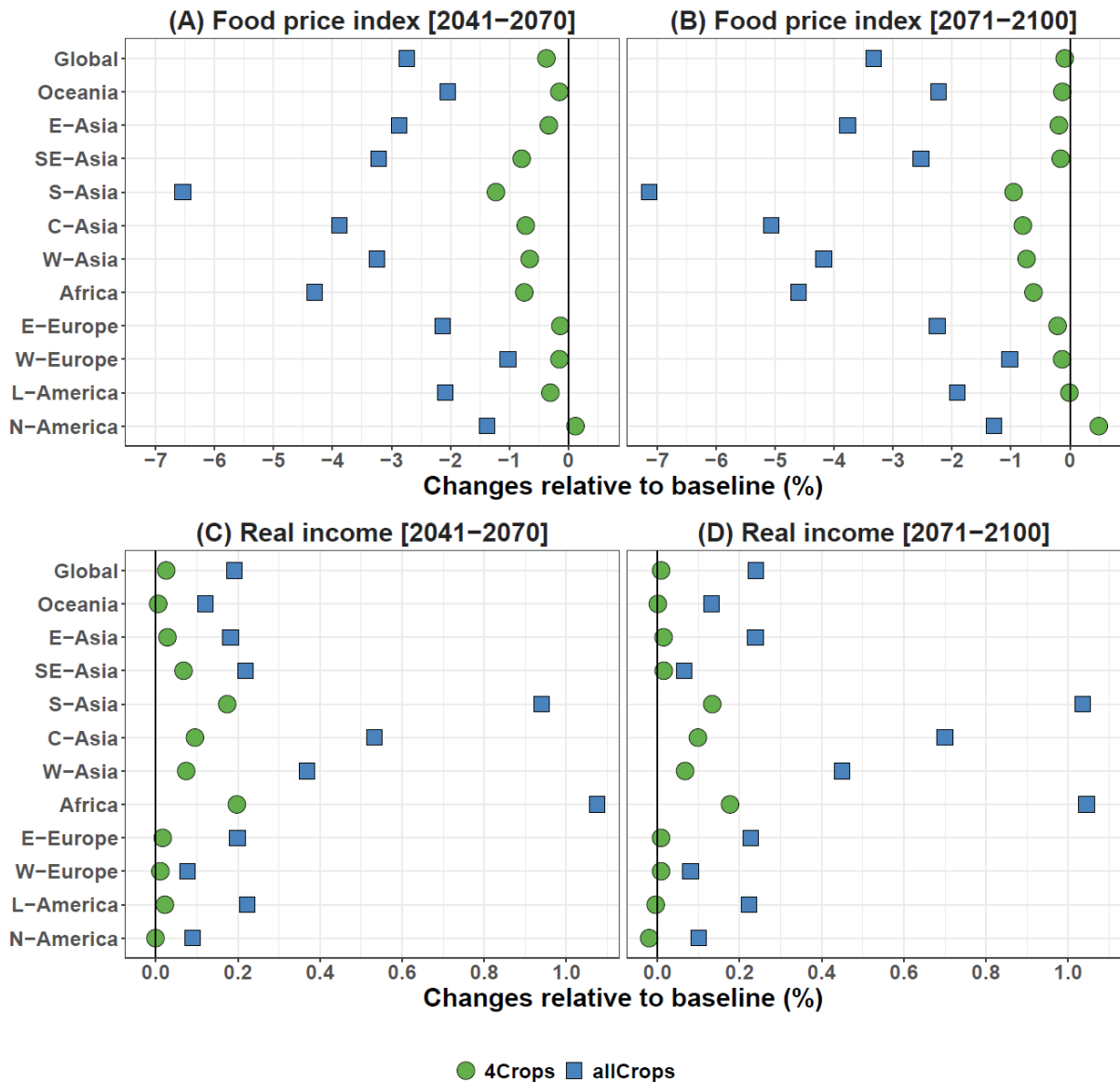


Fig. S9: Median responses of the food price index by the mid [2041–2070] (A) and end [2071–2100] (B) of the century, and regional real income by the mid [2041–2070] (C) and end [2071–2100] (D) of the century under RCP7.0 relative to the historical time period. The income responses are simulated using the GRACE model and show the median changes over GCMs and crop models relative to the state of the world economy in 2011. Heat stress impacts on labour are not included. The green circles show the scenarios that only consider the climate-related yield responses of for major crops. The blue squares show the scenario that consider the climate-related yield responses of all types of crops.

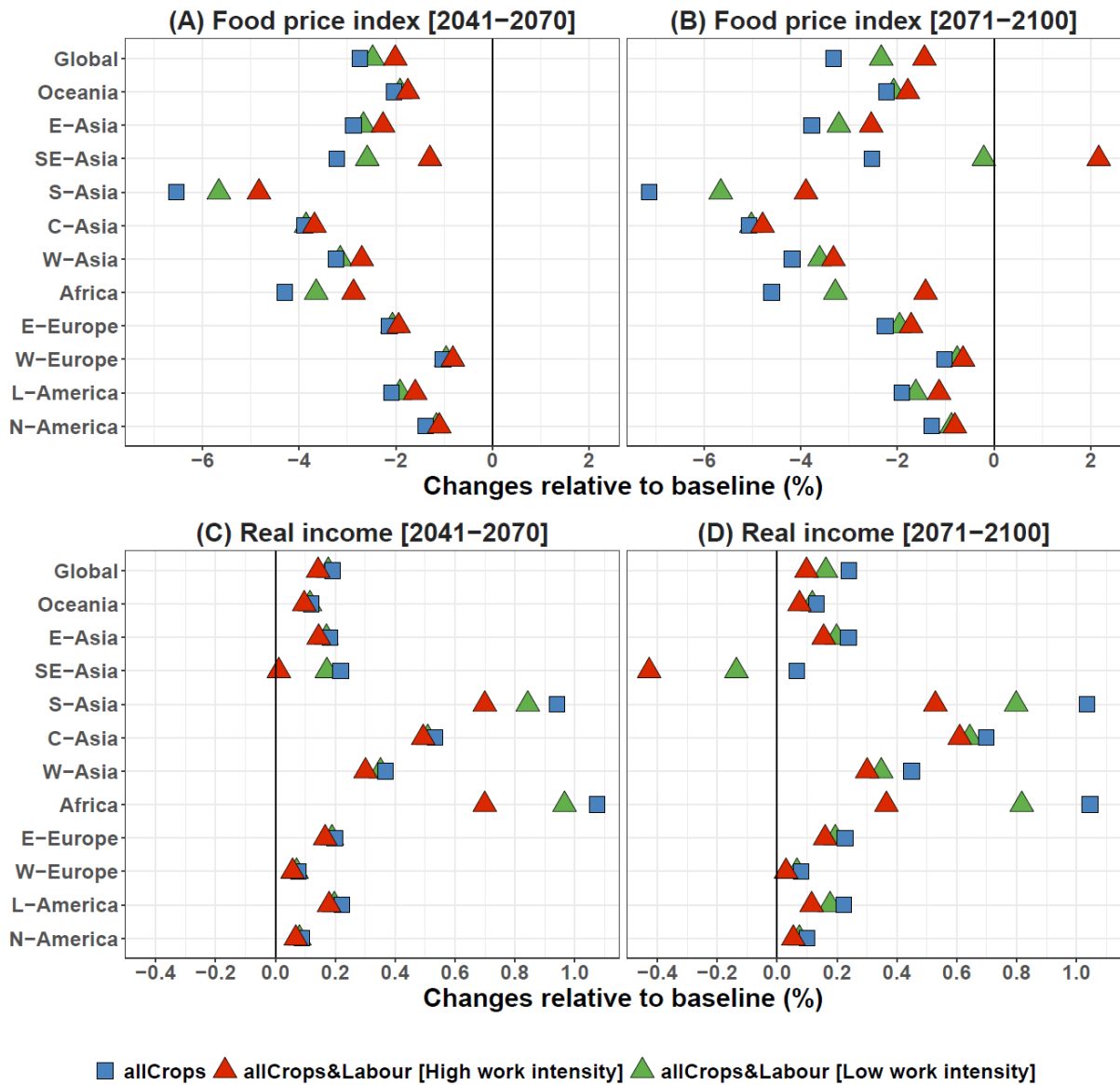


Fig. S10: Median responses of the food price index by the mid [2041–2070] (A) and end [2071–2100] (B) of the century, and regional real income by the mid [2041–2070] (C) and end [2071–2100] (D) of the century under RCP7.0 relative to the historical time period. The income responses are simulated using the GRACE model and show the median changes over GCMs, crop models, and heat-labour exposure-response functions relative to the state of the world economy in 2011. The blue squares show the scenarios that only consider the climate-related yield responses of all types of crops. The red triangles show the scenario that consider both yield changes and heat stress impacts on labour with high work intensity. The orange triangles are the same as the former but with a radical mechanisation deployment in crop production.

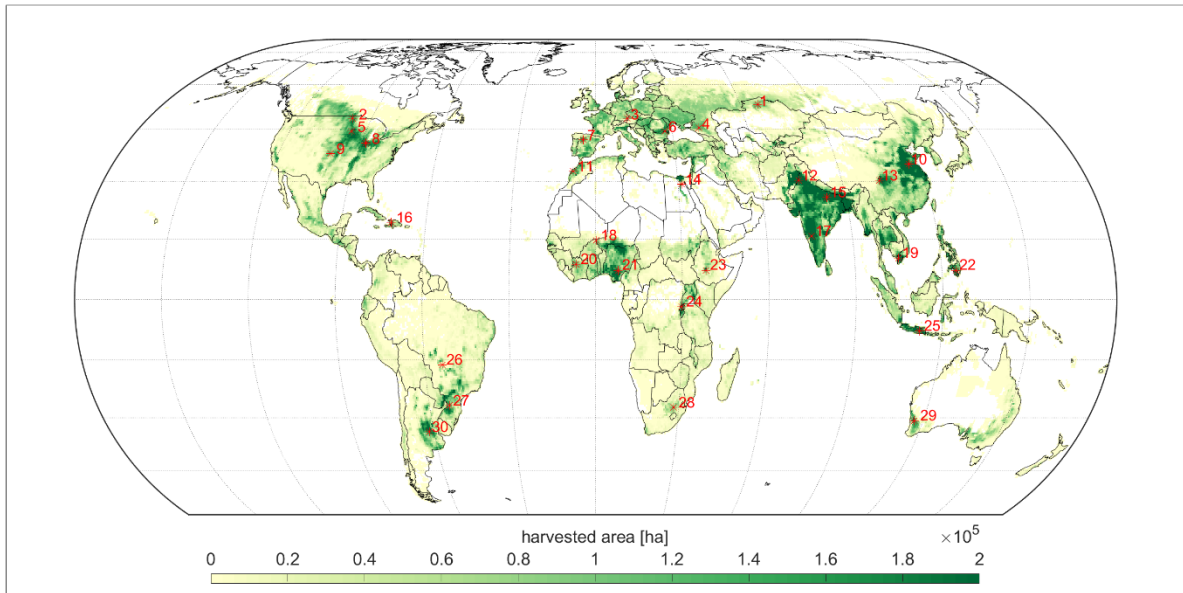


Fig. S11: Sample members selected to compare the levels of labour capacity which are calculated using hourly and daily mean climate data.

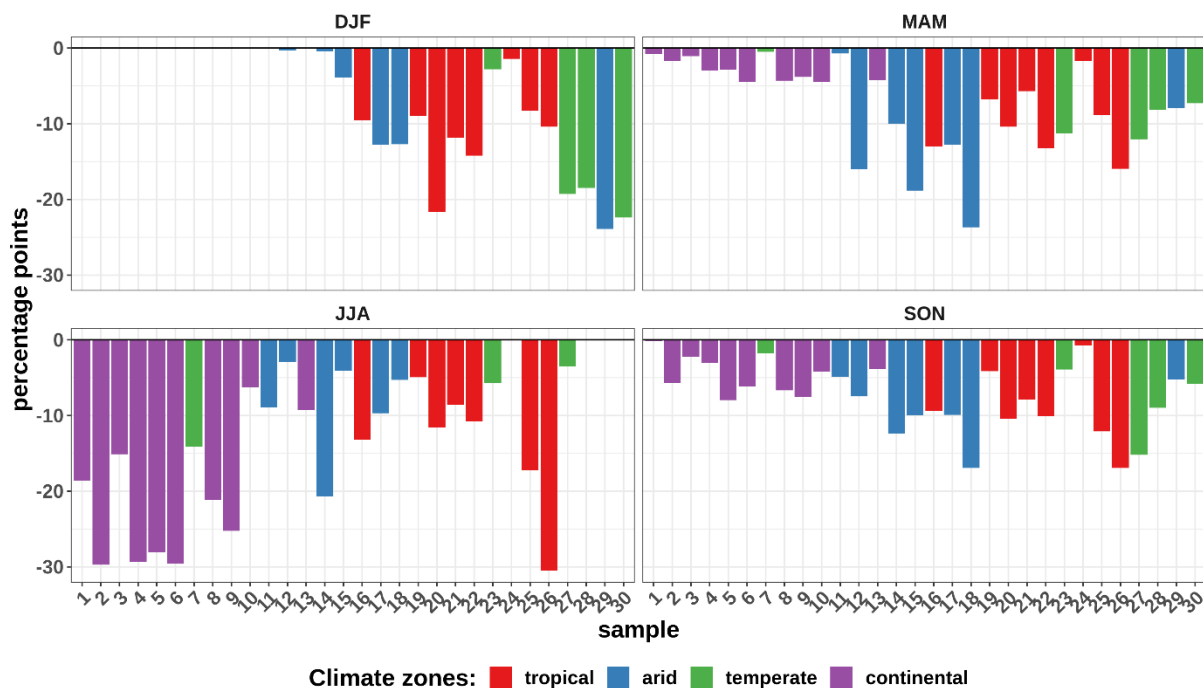


Fig. S12: Absolute differences between the levels of labour capacity calculated using hourly climate data for a 7 a.m. to 7 p.m. workday and those calculated using daily mean values of UKESM1-0-LL by the end of the century [2071–2100] under RCP7.0. The X-axis indicates the sample members (Fig. S11), which are ordered by latitude. Negative values show that when using hourly climate data, the labour capacity is smaller compared to when daily mean values of climate data are used. Labour capacity is estimated using the NIOSH exposure-response functions.

Supplemental References:

1. Zabel, F., and Poschlo, B. (2023). The Teddy tool v1.1: temporal disaggregation of daily climate model data for climate impact analysis. *Geosci. Model Dev.* *16*, 5383–5399. <https://doi.org/10.5194/gmd-16-5383-2023>.
2. Luckmann, J., Grethe, H., McDonald, S., Orlov, A., and Siddig, K. (2014). An integrated economic model of multiple types and uses of water. *Water Resour. Res.* *50*, 3875–3892. <https://doi.org/10.1002/2013WR014750>.
3. Orlov, A., Daloz, A.S., Sillmann, J., Thiery, W., Douzal, C., Lejeune, Q., and Schleussner, C. (2021). Global Economic Responses to Heat Stress Impacts on Worker Productivity in Crop Production. *Econ. Disasters Clim. Change*. <https://doi.org/10.1007/s41885-021-00091-6>.
4. Arrow, K.J., Chenery, H.B., Minhas, B.S., and Solow, R.M. (1961). Capital-Labor Substitution and Economic Efficiency. *Rev. Econ. Stat.* *43*, 225–250. <https://doi.org/10.2307/1927286>.
5. Gechert, S., Havranek, T., Irsova, Z., and Kolcunova, D. (2022). Measuring capital-labor substitution: The importance of method choices and publication bias. *Rev. Econ. Dyn.* *45*, 55–82. <https://doi.org/10.1016/j.red.2021.05.003>.
6. Antoszewski, M. (2019). Wide-range estimation of various substitution elasticities for CES production functions at the sectoral level. *Energy Econ.* *83*, 272–289. <https://doi.org/10.1016/j.eneco.2019.07.016>.

7. Knoblach, M., Roessler, M., and Zwerschke, P. (2020). The Elasticity of Substitution Between Capital and Labour in the US Economy: A Meta-Regression Analysis. *Oxf. Bull. Econ. Stat.* 82, 62–82. <https://doi.org/10.1111/obes.12312>.
8. Mućk, J. (2017). Elasticity of substitution between labor and capital: robust evidence from developed economies. NBP Work. Pap.
9. Calzadilla, A., Rehdanz, K., and Tol, R.S.J. (2011). The GTAP-W model: Accounting for water use in agriculture (Kiel Institute for the World Economy (IfW)).
10. Philip, J.-M., Sánchez-Chóliz, J., and Sarasa, C. (2014). Technological change in irrigated agriculture in a semiarid region of Spain. *Water Resour. Res.* 50, 9221–9235. <https://doi.org/10.1002/2014WR015728>.
11. Hertel, T., and Liu, J. (2019). Implications of Water Scarcity for Economic Growth. In *Economy-Wide Modeling of Water at Regional and Global Scales Advances in Applied General Equilibrium Modeling*, G. Wittwer, ed. (Springer), pp. 11–35. https://doi.org/10.1007/978-981-13-6101-2_2.
12. Hertel, T.W., Golub, A.A., Jones, A.D., O’Hare, M., Plevin, R.J., and Kammen, D.M. (2010). Effects of US Maize Ethanol on Global Land Use and Greenhouse Gas Emissions: Estimating Market-mediated Responses. *BioScience* 60, 223–231. <https://doi.org/10.1525/bio.2010.60.3.8>.
13. Keeney, R., and Hertel, T.W. (2009). The Indirect Land Use Impacts of United States Biofuel Policies: The Importance of Acreage, Yield, and Bilateral Trade Responses. *Am. J. Agric. Econ.* 91, 895–909.
14. Palatnik, R.R., Eboli, F., Ghermandi, A., Kan, I., Rapaport-Rom, M., and Shechter, M. (2011). Integration of general and partial equilibrium agricultural land-use transformation for the analysis of climate change in the mediterranean. *Clim. Change Econ.* 02, 275–299. <https://doi.org/10.1142/S2010007811000310>.
15. Zhao, X., van der Mensbrugghe, D.Y., Keeney, R.M., and Tyner, W.E. (2019). Improving the way land use change is handled in economic models. *Econ. Model.* <https://doi.org/10.1016/j.econmod.2019.03.003>.
16. Gaasland, I. (2008). Modelling farmers’ labour supply in CGE models (SNF).
17. Aaheim, H.A., Orlov, A., Wei, T., and Glomsrød, S. (2018). GRACE model and applications. CICERO Center for International Climate Research. Oslo, Norway. CICERO Reports; 2018:01. p. 1-45.
18. Mathiesen, L. (1985). Computation of economic equilibria by a sequence of linear complementarity problems. In *Economic Equilibrium: Model Formulation and Solution Mathematical Programming Studies*, A. S. Manne, ed. (Springer), pp. 144–162. <https://doi.org/10.1007/BFb0121030>.
19. Rutherford, T.F. (1995). Extension of GAMS for complementarity problems arising in applied economic analysis. *J. Econ. Dyn. Control* 19, 1299–1324. [https://doi.org/10.1016/0165-1889\(94\)00831-2](https://doi.org/10.1016/0165-1889(94)00831-2).